



**IJOER**  
RESEARCH JOURNAL

ISSN  
2395-6992

# International Journal of Engineering Research & Science



[www.ijoer.com](http://www.ijoer.com)  
[www.adpublications.org](http://www.adpublications.org)

## Preface

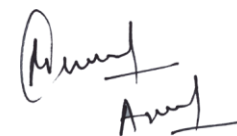
We would like to present, with great pleasure, the inaugural volume-5, Issue-6, June 2019, of a scholarly journal, *International Journal of Engineering Research & Science*. This journal is part of the AD Publications series *in the field of Engineering, Mathematics, Physics, Chemistry and science Research Development*, and is devoted to the gamut of Engineering and Science issues, from theoretical aspects to application-dependent studies and the validation of emerging technologies.

This journal was envisioned and founded to represent the growing needs of Engineering and Science as an emerging and increasingly vital field, now widely recognized as an integral part of scientific and technical investigations. Its mission is to become a voice of the Engineering and Science community, addressing researchers and practitioners in below areas

Chemical Engineering	
Biomolecular Engineering	Materials Engineering
Molecular Engineering	Process Engineering
Corrosion Engineering	
Civil Engineering	
Environmental Engineering	Geotechnical Engineering
Structural Engineering	Mining Engineering
Transport Engineering	Water resources Engineering
Electrical Engineering	
Power System Engineering	Optical Engineering
Mechanical Engineering	
Acoustical Engineering	Manufacturing Engineering
Optomechanical Engineering	Thermal Engineering
Power plant Engineering	Energy Engineering
Sports Engineering	Vehicle Engineering
Software Engineering	
Computer-aided Engineering	Cryptographic Engineering
Teletraffic Engineering	Web Engineering
System Engineering	
Mathematics	
Arithmetic	Algebra
Number theory	Field theory and polynomials
Analysis	Combinatorics
Geometry and topology	Topology
Probability and Statistics	Computational Science
Physical Science	Operational Research
Physics	
Nuclear and particle physics	Atomic, molecular, and optical physics
Condensed matter physics	Astrophysics
Applied Physics	Modern physics
Philosophy	Core theories

Chemistry	
Analytical chemistry	Biochemistry
Inorganic chemistry	Materials chemistry
Neurochemistry	Nuclear chemistry
Organic chemistry	Physical chemistry
Other Engineering Areas	
Aerospace Engineering	Agricultural Engineering
Applied Engineering	Biomedical Engineering
Biological Engineering	Building services Engineering
Energy Engineering	Railway Engineering
Industrial Engineering	Mechatronics Engineering
Management Engineering	Military Engineering
Petroleum Engineering	Nuclear Engineering
Textile Engineering	Nano Engineering
Algorithm and Computational Complexity	Artificial Intelligence
Electronics & Communication Engineering	Image Processing
Information Retrieval	Low Power VLSI Design
Neural Networks	Plastic Engineering

Each article in this issue provides an example of a concrete industrial application or a case study of the presented methodology to amplify the impact of the contribution. We are very thankful to everybody within that community who supported the idea of creating a new Research with IJOER. We are certain that this issue will be followed by many others, reporting new developments in the Engineering and Science field. This issue would not have been possible without the great support of the Reviewer, Editorial Board members and also with our Advisory Board Members, and we would like to express our sincere thanks to all of them. We would also like to express our gratitude to the editorial staff of AD Publications, who supported us at every stage of the project. It is our hope that this fine collection of articles will be a valuable resource for *IJOER* readers and will stimulate further research into the vibrant area of Engineering and Science Research.



Mukesh Arora  
(Chief Editor)

## **Board Members**

### **Mukesh Arora(Editor-in-Chief)**

BE(Electronics & Communication), M.Tech(Digital Communication), currently serving as Assistant Professor in the Department of ECE.

### **Prof. Dr. Fabricio Moraes de Almeida**

Professor of Doctoral and Master of Regional Development and Environment - Federal University of Rondonia.

### **Prof.S.Balamurugan**

Department of Information Technology, Kalaignar Karunanidhi Institute of Technology, Coimbatore, Tamilnadu, India.

### **Dr. Omar Abed Elkareem Abu Arqub**

Department of Mathematics, Faculty of Science, Al Balqa Applied University, Salt Campus, Salt, Jordan, He received PhD and Msc. in Applied Mathematics, The University of Jordan, Jordan.

### **Dr. AKPOJARO Jackson**

Associate Professor/HOD, Department of Mathematical and Physical Sciences, Samuel Adegboyega University, Ogwa, Edo State.

### **Dr. Ajoy Chakraborty**

Ph.D.(IIT Kharagpur) working as Professor in the department of Electronics & Electrical Communication Engineering in IIT Kharagpur since 1977.

### **Dr. Ukar W.Soelistijo**

Ph D , Mineral and Energy Resource Economics, West Virginia State University, USA, 1984, Retired from the post of Senior Researcher, Mineral and Coal Technology R&D Center, Agency for Energy and Mineral Research, Ministry of Energy and Mineral Resources, Indonesia.

### **Dr. Samy Khalaf Allah Ibrahim**

PhD of Irrigation &Hydraulics Engineering, 01/2012 under the title of: "Groundwater Management Under Different Development Plans In Farafra Oasis, Western Desert, Egypt".

### **Dr. Ahmet ÇİFCİ**

Ph.D. in Electrical Engineering, Currently Serving as Head of Department, Burdur Mehmet Akif Ersoy University, Faculty of Engineering and Architecture, Department of Electrical Engineering (2015-...)

### **Dr. Heba Mahmoud Mohamed Afify**

Ph.D degree of philosophy in Biomedical Engineering, Cairo University, Egypt worked as Assistant Professor at MTI University.

## **Dr. Aurora Angela Pisano**

Ph.D. in Civil Engineering, Currently Serving as Associate Professor of Solid and Structural Mechanics (scientific discipline area nationally denoted as ICAR/08"-"Scienza delle Costruzioni"), University Mediterranea of Reggio Calabria, Italy.

## **Dr. Faizullah Mahar**

Associate Professor in Department of Electrical Engineering, Balochistan University Engineering & Technology Khuzdar. He is PhD (Electronic Engineering) from IQRA University, Defense View, Karachi, Pakistan.

## **Dr. S. Kannadhasan**

Ph.D (Smart Antennas), M.E (Communication Systems), M.B.A (Human Resources).

## **Dr. Christo Ananth**

Ph.D. Co-operative Networks, M.E. Applied Electronics, B.E Electronics & Communication Engineering Working as Associate Professor, Lecturer and Faculty Advisor/ Department of Electronics & Communication Engineering in Francis Xavier Engineering College, Tirunelveli.

## **Dr. S.R.Boselin Prabhu**

Ph.D, Wireless Sensor Networks, M.E. Network Engineering, Excellent Professional Achievement Award Winner from Society of Professional Engineers Biography Included in Marquis Who's Who in the World (Academic Year 2015 and 2016). Currently Serving as Assistant Professor in the department of ECE in SVS College of Engineering, Coimbatore.

## **Dr. Maheshwar Shrestha**

Postdoctoral Research Fellow in DEPT. OF ELE ENGG & COMP SCI, SDSU, Brookings, SD  
Ph.D, M.Sc. in Electrical Engineering from SOUTH DAKOTA STATE UNIVERSITY, Brookings, SD.

## **Zairi Ismael Rizman**

Senior Lecturer, Faculty of Electrical Engineering, Universiti Teknologi MARA (UiTM) (Terengganu) Malaysia  
Master (Science) in Microelectronics (2005), Universiti Kebangsaan Malaysia (UKM), Malaysia. Bachelor (Hons.) and Diploma in Electrical Engineering (Communication) (2002), UiTM Shah Alam, Malaysia

## **Dr. D. Amaranatha Reddy**

Ph.D.(Postdoctoral Fellow,Pusan National University, South Korea), M.Sc., B.Sc. : Physics.

## **Dr. Dibya Prakash Rai**

Post Doctoral Fellow (PDF), M.Sc.,B.Sc., Working as Assistant Professor in Department of Physics in Pachhungga University College, Mizoram, India.

## **Dr. Pankaj Kumar Pal**

Ph.D R/S, ECE Deptt., IIT-Roorkee.

## **Dr. P. Thangam**

BE(Computer Hardware & Software), ME(CSE), PhD in Information & Communication Engineering, currently serving as Associate Professor in the Department of Computer Science and Engineering of Coimbatore Institute of Engineering and Technology.

## **Dr. Pradeep K. Sharma**

PhD., M.Phil, M.Sc, B.Sc, in Physics, MBA in System Management, Presently working as Provost and Associate Professor & Head of Department for Physics in University of Engineering & Management, Jaipur.

## **Dr. R. Devi Priya**

Ph.D (CSE),Anna University Chennai in 2013, M.E, B.E (CSE) from Kongu Engineering College, currently working in the Department of Computer Science and Engineering in Kongu Engineering College, Tamil Nadu, India.

## **Dr. Sandeep**

Post-doctoral fellow, Principal Investigator, Young Scientist Scheme Project (DST-SERB), Department of Physics, Mizoram University, Aizawl Mizoram, India- 796001.

## **Mr. Abilash**

M.Tech in VLSI, B.Tech in Electronics & Telecommunication engineering through A.M.I.E.T.E from Central Electronics Engineering Research Institute (C.E.E.R.I) Pilani, Industrial Electronics from ATI-EPI Hyderabad, IEEE course in Mechatronics, CSHAM from Birla Institute Of Professional Studies.

## **Mr. Varun Shukla**

M.Tech in ECE from RGPV (Awarded with silver Medal By President of India), Assistant Professor, Dept. of ECE, PSIT, Kanpur.

## **Mr. Shrikant Harle**

Presently working as a Assistant Professor in Civil Engineering field of Prof. Ram Meghe College of Engineering and Management, Amravati. He was Senior Design Engineer (Larsen & Toubro Limited, India).

## Table of Contents

S.No	Title	Page No.
1	<p><b>A Quasi Experimental Study to Assess the Effectiveness of Planned Teaching Programme on Knowledge of Primary School Teachers Regarding Selected Emotional and Behavioural Disorders of Children in Selected School of Karauli District Rajasthan</b></p> <p><b>Authors:</b> Mr. Bal Kishan Jangid, Dr. Rahul Tiwari, Mr. Vikas Choudhary</p> <p> <b>DOI:</b> 10.5281/zenodo.3264031</p> <p> <b>DIN Digital Identification Number:</b> IJOER-JUN-2019-1</p>	01-10
2	<p><b>Free-Radical Nonbranched-Chain Hydrogen Oxidation</b></p> <p><b>Authors:</b> Michael M. Silaev</p> <p> <b>DOI:</b> 10.5281/zenodo.3264033</p> <p> <b>DIN Digital Identification Number:</b> IJOER-JUN-2019-3</p>	11-20
3	<p><b>Zig-zag theories differently accounting for layerwise effects of multilayered composites</b></p> <p><b>Authors:</b> Andrea Urraci, Ugo Icardi</p> <p> <b>DOI:</b> 10.5281/zenodo.3264035</p> <p> <b>DIN Digital Identification Number:</b> IJOER-JUN-2019-9</p>	21-42

# “A Quasi Experimental Study to Assess the Effectiveness of Planned Teaching Programme on Knowledge of Primary School Teachers Regarding Selected Emotional and Behavioural Disorders of Children in Selected School of Karauli District Rajasthan”

Mr. Bal Kishan Jangid<sup>1</sup>, Dr. Rahul Tiwari<sup>2</sup>, Mr. Vikas Choudhary<sup>3</sup>

<sup>1</sup>Ph.D Scholar, MVGU, Jaipur

<sup>2</sup>Guide, MVGU, Jaipur

<sup>3</sup>Ph.D Scholar, MVGU, Jaipur

**Abstract**— The finding of the present study were analyzed and discussed with finding of similar studies. This helped the investigator to prove that the findings were true and the planned teaching programme was effective in improving knowledge of Primary School Teachers. It included statement, objective, assumption, hypothesis and tool used for the study and findings.

The study made use of a quasi- experimental approach with one group pre-test and post-test design. The population of the study consisted of Primary School Teachers at selected school of Alwar. Convenient sampling technique was utilized to select 158 Primary School Teachers based on certain pre-determined criteria.

**Keywords**— Emotional behavior disorder, behavioral disorder, karauli district study, children early age growth, children behavior, health care of children.

## I. INTRODUCTION

### 1.1 Background of Study

The early years of a child's life are very important for his or her health and development. Healthy development means that children of all abilities, including those with special health care needs, are able to grow up where their social, emotional and educational needs are met. Having a safe and loving home and spending time with family—playing, singing, reading, and talking—are very important. Proper nutrition, exercise, and sleep also can make a big difference.

#### 1.1.1 Emotional and Behavior Disorders (EBD)

Emotional and Behavioral Disorders (EBD) are typically referred to when a child is experiencing emotional disorders having behavioral issues. Emotional and Behavior Disorders, is also referred to as Emotional and Behavioral Disorders, Behavioral and Emotional Disorders, Mental and Behavioral Disorders, and Emotional Behavioral Disability, also abbreviated EBD. In the criteria for special education for children aged 3 to 12 years, "emotional disturbance" is one of the eligible disabilities.

Emotional and Behavioral Disorder (EBD) refers to a condition in which behavioral or emotional responses of an individual in school are so different from his/her generally accepted age appropriate, ethnic or cultural norms that it adversely affects performance in such areas as self care, social relationships, personal adjustment, academic progress and classroom behavior or work adjustment (Forness & Knitzer.,1992). EBD is mainly divided into three types: Attention Deficit Disorder (ADD), Anxiety Disorder and Conduct Disorder.

### 1.1.2 EBD and ICD

Section F90-F98 of the ICD-10, which has the title mentioned above tying it to our topic, contains seven categories of disorders. Here they are, with clarifying examples of the subtopics:

- Hyperkinetic disorders, including Attention-deficit hyperactivity disorder (ADHD)
- Conduct disorders, including those confined to the family, those not so confined, and Oppositional Defiant Disorder (ODD)
- Mixed disorders of conduct and emotions, including Depressive Conduct Disorder
- Emotional disorders with onset specific to childhood, including separation anxiety disorder, sibling rivalry disorder, and social anxiety disorder
- Disorders of social functioning with onset specific to childhood and adolescence, including elective or selective mutism
- Tic disorders, including Tourette's Disorder
- Other behavioral and emotional disorders with onset usually occurring in childhood and adolescence, including stuttering, pica, cluttering, thumb-sucking, and Attention Deficit Disorder without hyperactivity (ADD).

### 1.1.3 EBD and DSM-IVR

The DSM-IVR has a different organizational system for the most closely corresponding section, which it calls "Disorders usually first diagnosed in infancy, childhood, or adolescence." First, it includes learning disabilities that are clearly not emotional or behavioral disorders or disabilities, like autism and mental retardation. In addition, EBD disorders are not sorted out from other disabilities and placed in separate categories, as you will see in this summary of the seven categories that contain EBD disorders:

- Communication disorders including not only stuttering, but also expressive language disorder (which the ICD categorizes as a disorder of psychological development)
- Attention-deficit and disruptive behavior disorders, including ADHD, Conduct Disorder, and Oppositional Defiant Disorder (ODD)
- Feeding and eating disorders of infancy or early childhood, including pica
- Tic disorders, including Tourette's Disorder
- Elimination disorders
- Other disorders of infancy, childhood, or adolescence, including separation anxiety disorder and selective Mutism

## 1.2 Need of the Study

### 1.2.1 Mental Sickness In Children In India : An Overview

Research from the Indian Council of Medical Research reported that **12% children between 4 to 16 years suffered from psychiatric disorders** in India. Similar studies from around the globe supported the fact that around 15% children suffer from significant mental health problems, affecting their social and physical functioning. Global studies show (Published in June 2011 of *The Lancet*) that one in every two adolescents globally suffers from neuro-psychiatric disorders. It further added that, one in five adolescents has an emotional, learning or development disorder while one in every eight has a serious mental disorder.

### 1.2.2 Some Facts Pertaining To Mental Illness in Children

- Most common causes of disorders especially in adolescents could be depression, alcohol abuse, schizophrenia and bipolar disorders
- Other studies show close to **20 % Indian children suffer from some form of mental disorder**, of which about **2-5 % is serious disorders including cases like autism, Schizophrenia** etc. - which could also be at different levels.
- Irritability, sleeping and eating disorders and obsessive compulsive disorders that seem insignificant to most, if ignored, could also later manifest as more serious concerns.
- WHO has estimated that by 2020, mental depression will be the largest cause of disability worldwide **By 2025, mental illness will catch up with heart disease or may even overtake it as the biggest global health concern.**
- **Only 1 in 50 people with mental health problems have access to treatment in developing countries** (and 1 in 3 in wealthy nations).
- India is awfully short of psychiatrists with just 4,000 present all over the country. **District mental health programmes are placed in only 123 of 640 districts, with total coverage anticipated only by 2017.**
- As per the National Mental Health Survey, 2015 conducted by WHO, 1 in 20 children in India suffer from mental disorder. The prevalence of mental disorders in the 5-12 age group was 7.3%. As per the report, nearly 9.8 million young Indians in the age group 13-17 were in need of active intervention. The prevalence of mental disorder was almost twice in urban areas (13.5%) in comparison to rural areas (6.9%). Some of the most common prevalent problems were Attention Deficit Disorder (1.8%), Intellectual Disability (1.7%), Autism Spectrum Disorder (1.6%), Phobic anxiety disorder (1.3%) and Psychotic disorder (1.3%).

## II. OBJECTIVES OF THE STUDY

- To assess the knowledge level of **Primary School Teachers** regarding selected emotional and behavioural disorders of children.
- To find out the association between pre-test knowledge and selected demographic variables of **Primary School Teachers** regarding selected emotional and behavioural disorders of children.
- To evaluate the effectiveness of planned teaching programme on knowledge of **Primary School Teachers** regarding selected emotional and behavioural disorders of children.

## III. METHODOLOGY

**Research approach:** - Quasi experimental Research approach was used.

**Research design:** - Quasi experimental, one group pre- test and post-test design was used.

**TABLE: 1**  
**SCHEMATIC REPRESENTATION OF THE STUDY DESIGN**

Pre-test (Day 1)	Administration of Planned Teaching Programme	Post – test (After 7 Day)
O1	X	O2

*O1 = Pre-test knowledge on first day.*

*X = Intervention was Planned Teaching Program on first day.*

*O2 = Post-test knowledge after Seventh day.*

The schematic representation of the study design shows that study was conducted in three phases and represented in figure number- 1.

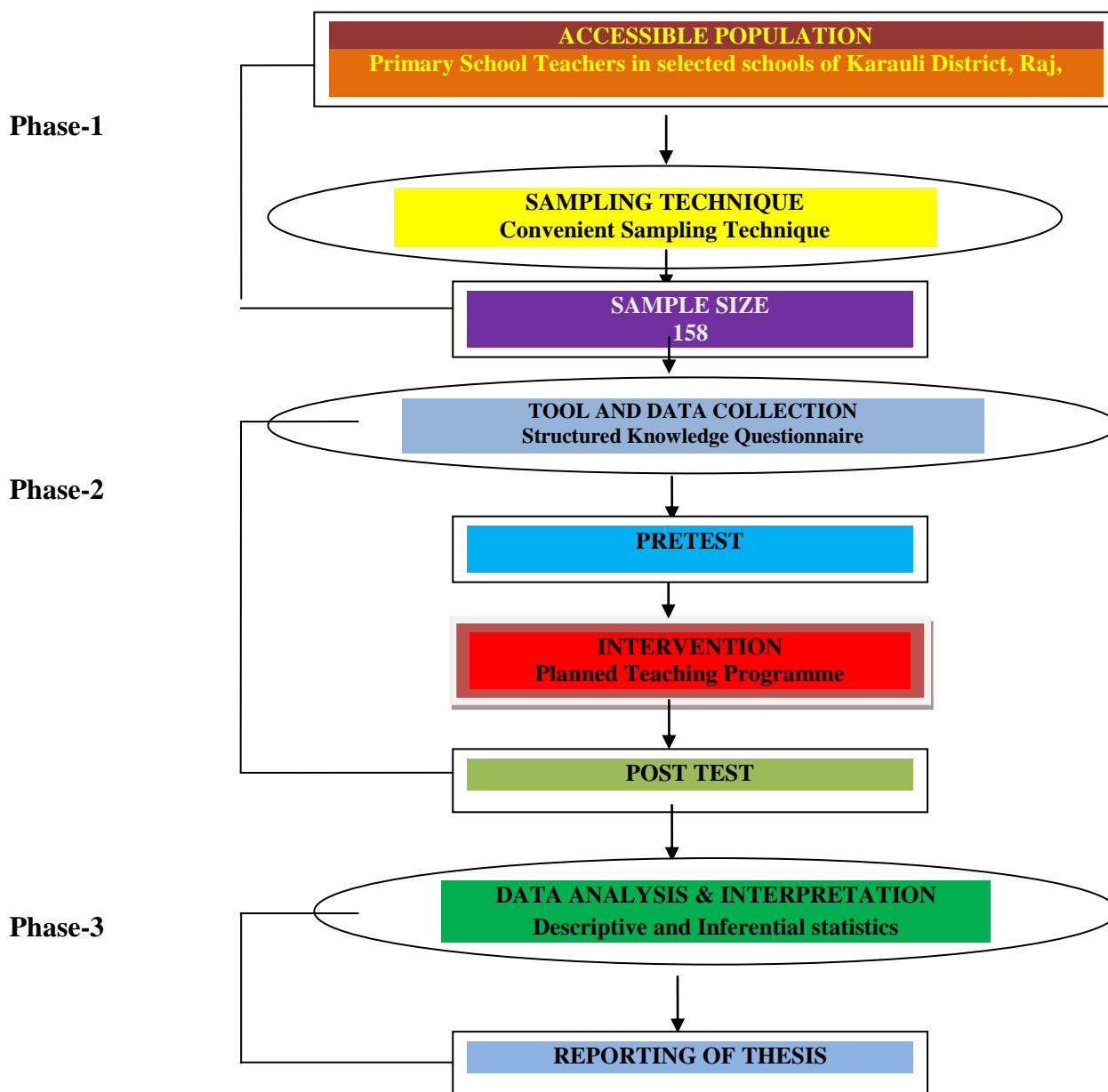


FIG 1. Schematic presentation of Research Design

3.1 Variables

**Independent variables:** - Independent variable in the study was the Plan Teaching Program.

**Dependent variables:** - Dependent variable in the study was Knowledge regarding selected emotional and behavioral disorders of children.

**Extraneous variable:** In this study, extraneous variable refers to such as age, educational status, marital status, income, teaching experience etc.

**Setting:-**This study was conducted in Rajni Public School, Danal Pur, Vishkarma Public School, Shri Mahaveer Ji, Adarsh Public School, Shri Mahaveer Ji, Gyandeep Sr. Sec. School, Banwari Pur, Kamla Devi Sr. Sec. School, Banwari Pur, Jai

Ambey Sr. Sec. School, Banwari Pur Mod, Shrimahaveer Ji, etc. Karauli District, Rajasthan.

**Population:** - The population was Primary School Teachers, who were working in selected primary schools of Karauli District, Rajasthan.

**Sample:** - Sample consists of Primary School Teachers.

**Sampling techniques:** - Convenient sampling technique was used to select the sample

**Sample size:** - sample size comprised of 158 Primary School Teachers

**Development and description of tool:** - The tool was developed by –Review of literature which provided adequate content area and information. Consultation and discussion with experts from nursing, psychologists and psychiatry and Personal experiences of the investigator were an added advantage for tool development.

#### **Description of final tool**

The final tool used in the study consists of four sections:

Section –A: Demographic variable

Section-B Structured Knowledge questionnaire regarding Attention deficit hyperactive disorder

Section –C structured knowledge questionnaire on Anxiety disorder

Section –D structure knowledge questionnaire on conduct disorder

Each item in the tool consisted of multiple choice questions to respondents and were requested to place tick mark (✓) against one single answer for each question and each question carried one score. The maximum total score of the questionnaire was 24.

Score was graded as follows- Good (17-24 scores), Average (9-16 scores) and Poor (0-8scores)

**Validation of the tool:** - The tool was validated by 5 experts from psychiatric nursing specialty, and other 2 were psychologists and 2 were psychiatrists.

**Reliability of tool:** - The reliability of the tool obtained 0.89 by Karl Spearman prophecy formula proved that the tool was reliable.

**Procedure for data collection:** - Written permission was obtained from the concerned authorities before data collection. The investigator established rapport with Primary School Teachers and obtained an informed written consent after explaining the importance and purpose of the study. Pretest questionnaire was administered to Primary School Teachers. The data was collected by structured Knowledge questionnaire tool. Average time taken for pretest was 20-25 minutes. Planned teaching programme was given to the group of Primary School Teachers. The Post test was obtained on after 7<sup>th</sup> day of the pre-test by administering the same knowledge questionnaire.

## **IV. RESULTS**

The collected data from the Primary School Teachers are organized and presented under the following sections:-

### **4.1 Section I: Description of Socio-Demographic Variables of Primary School Teachers**

**TABLE-2**  
**FREQUENCY AND PERCENTAGE DISTRIBUTION OF SUBJECTS ACCORDING TO SOCIO- DEMOGRAPHIC VARIABLES.**

N=158

S. No.	Demographic variables	Frequency(N)	Percentage (%)
1	<b>Age in years</b>		
	• <25 Yrs	17	10.75
	• 25-30 Yrs	49	31.01
	• 31-35 Yrs	53	33.54
	• > 35 Yrs	39	24.68
2	<b>Gender</b>		
	• Male	60	37.97
	• Female	98	62.02
3	<b>Religion</b>		
	• Hindu	98	62.02
	• Muslim	38	24.05
	• Christian	22	13.92
4	<b>Marital Status</b>		
	• Married	118	74.68
	• Unmarried	40	25.31
5	<b>Education</b>		
	• Master degree with B.Ed.	85	53.79
	• Master degree with M.Ed.	15	9.49
	• Undergraduate with B.Ed.	58	36.70
6	<b>Teaching experience in number of years</b>		
	• <10 Yrs	56	35.44
	• 10-20 Yrs	84	53.16
	• 20-30 Yrs	14	8.86
	• > 30 Yrs	4	2.53
7	<b>Income</b>		
	• <10000	64	40.50
	• 10001 - 20000	56	35.44
	• 20001 – 30000	25	15.82
	• >30001	13	8.22
8	<b>Attended in-service education programme on Emotional and Behavioral Disorders of Children</b>		
	• Yes	9	5.69
	• No	149	94.90
9	<b>Resident area</b>		
	• Urban	93	58.86
	• Rural	65	41.13
10	<b>Refer if the child has Emotional and Behavioral Disorders</b>		
	• Psychiatrist	27	17.08
	• Psychologist	42	26.58
	• Child specialist	89	56.32

➤ Table 2 depict that the majority of 53 (33.54 %) Primary School Teachers in age group of 31-35 years and only 17 (10.75%) Primary School Teachers in the age group of < 25 years.

- It showed 62.02 % of Primary school teachers were females and 37.97% were male. Hence, it can be interpreted that most of the Primary School Teachers under study were females.
- Table- 2 reveals that majority of Primary School Teachers, 98 (62.2 %) belonged to Hindu and 38 (24.05%) belonged to Muslim religion. While 22(613.92 %) were from Christian religion.
- Table-2 show that 118 (74.68 %) Primary School Teachers were Married while 40 (25.31%) were Unmarried.
- It reveal that majority of Primary School Teachers, 85 (53.79%) were from Master degree with B.Ed and 58 (36.70 %) were from Undergraduate with B.Ed. and 15 (9.49 %) were from Master degree with M.Ed .
- Table 2 reveal that majority of Primary School Teachers, 84 (53.16 %) ,had 10 – 20 year teaching experience,56 (35.44%) had <10 year teaching experience,14 (8.86%) had 20 – 30 year experience and 4 (2.53 %) had > 30 year teaching experience.
- Table 2 show that the maximum number, 64 (40.50 %) and 56 (35.44 %) of Primary School Teachers had monthly income Rs. <10,000/- and Rs. 10,001/--20,000/ respectively. 25 Primary School Teachers (15.82 %) and 13 Primary School Teachers (8.22 %) had monthly income of Rs.20,001/- to 30,000 /- and More than Rs.30,001/respectively.
- Table 2 show that the most of Primary School Teachers, 93 (58.86 %) belonged to Urban Area and 65 (41.13 %) belonged to Rural Area.

**4.2 Section II: Assessment of Pretest Knowledge Regarding Emotional and Behavioural Problems Among Primary School Teachers**

Table 2 depicts that 85(53.79%) had poor knowledge, 65 (41.13%) had average knowledge and 8 (5.06%) had good knowledge regarding Emotional and Behavioral Disorders of children among Primary School Teachers.

**TABLE: -2**  
**PERCENTAGE DISTRIBUTIONS OF PRE-TEST KNOWLEDGE SCORE OF PRIMARY SCHOOL TEACHERS REGARDING SELECTED EMOTIONAL AND BEHAVIORAL DISORDERS OF CHILDREN**

Knowledge Score	Grade	Pretest			
		Frequency	Percentage	Mean score	S.D
0-8	Poor	85	53.79	8.60	±4.93
9-16	Average	65	41.13		
17-24	Good	8	5.06		

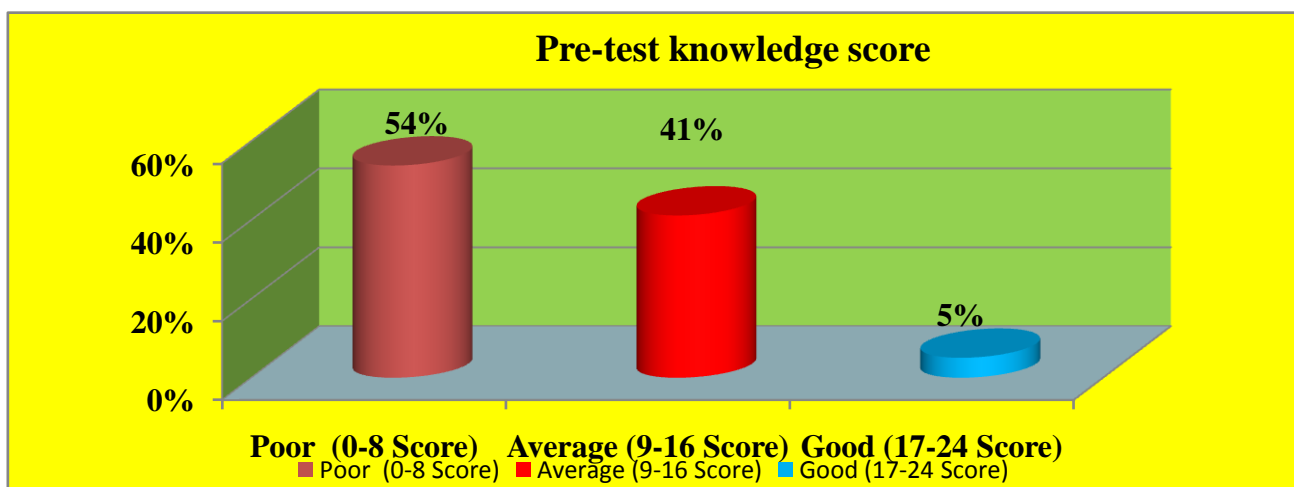


**FIGURE 2: Bar Diagram showing Pre-test knowledge score of Primary School Teachers regarding emotional and behaviour problems of children.**

**4.3 Section Iii: Assessment of Post Test Knowledge Regarding Selected Emotional And Behavioral Disorders Of Children Among Primary School Teachers.**

**TABLE: 3**  
**FREQUENCY AND PERCENTAGE DISTRIBUTION OF POST –TEST KNOWLEDGE REGARDING SELECTED EMOTIONAL AND BEHAVIORAL DISORDERS OF CHILDREN.**

N=158

Knowledge Score	Grade	Post-test			
		Frequency	Percentage	Mean score	S.D
0-8	Poor	0	0	15.34	±4.70
9-16	Average	96	60.75%		
17-24	Good	62	39.24%		

Table 3 depicts that after Planned Teaching Programme on the knowledge of the Primary School Teachers regarding the Emotional and Behavioral Disorders in children has increased to average 96 (60.75%) and good 62 (39.24%).

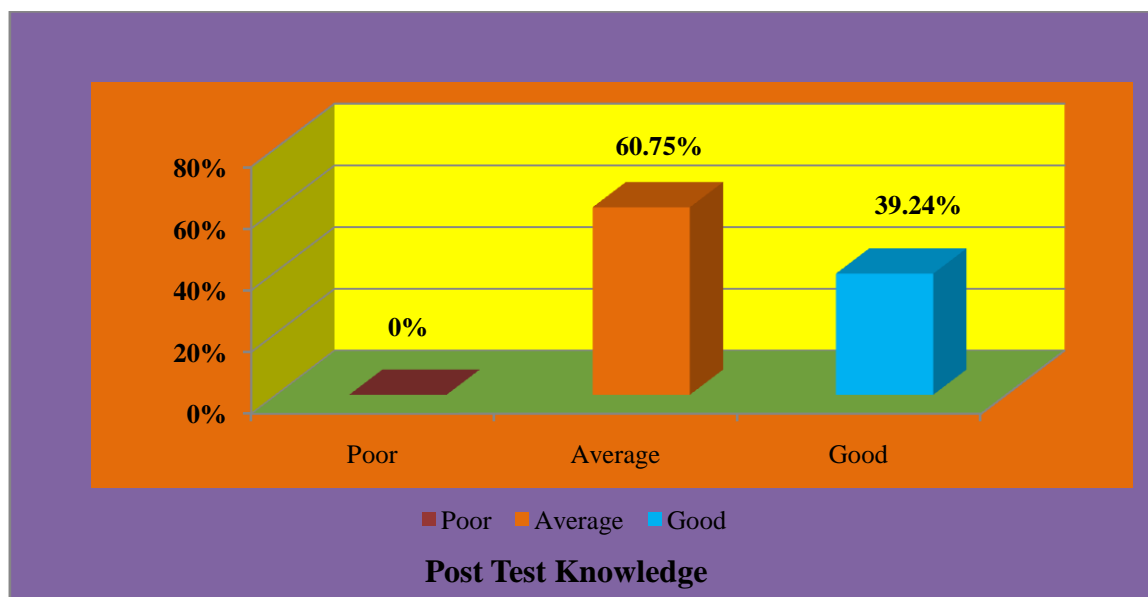


**FIGURE 3: Bar diagram showing the Post test knowledge score of Primary School Teachers regarding emotional and behavior problems of children.**

**4.4 Section IV-Association between Pretest Knowledge Score With Selected Socio-Demographic Variables.**

*Significant at the level of  $p < 0.05$ \**

Table No. 4 reveals that the computed chi-square value in all areas indicates no significant association between pre-test knowledge scores with Age ,Gender, Religion, Marital Status, Educational Qualification, Teaching experience , Income, Attended in-service education programme, Resident area etc. Hence research hypothesis  $H_2$  was rejected and null hypothesis  $H_{02}$  was accepted.

**TABLE NO. 4**  
**CHI-SQUARE VALUE SHOWING ASSOCIATION BETWEEN PRE-TEST KNOWLEDGE SCORES AND SELECTED**  
**SOCIO-DEMOGRAPHIC VARIABLES.**

N=158

S.No. No.	Demographic variables	Poor	Average	Good	df	$\chi^2$ Value
1	<b>Age in years</b> <ul style="list-style-type: none"> <li>• &lt;25 Yrs</li> <li>• 25-30 Yrs</li> <li>• 31-35 Yrs</li> <li>• &gt; 35 Yrs</li> </ul>	9 (6.32%) 26 (17.72%) 29 (20.25%) 21 (14.55%)	7 (4.43%) 21 (13.29%) 21 (13.29%) 16 (10.12%)	1 2 3 2	6	$\chi^2$ Value:0.2339 Not significant
2	<b>Gender</b> <ul style="list-style-type: none"> <li>• Male</li> <li>• Female</li> </ul>	32 (22.15) 53(36.70)	25 (15.82) 40(25.31)	3 5	2	$\chi^2$ Value:0.0112 Not significant
3	<b>Religion</b> <ul style="list-style-type: none"> <li>• Hindu</li> <li>• Muslim</li> <li>• Christian</li> </ul>	53 (36.70%) 20(13.92) 12 (8.22)	40 (25.31%) 16(10.12) 9(5.69)	5 2 1	4	$\chi^2$ Value:0.0397 Not significant
4	<b>Marital Status</b> <ul style="list-style-type: none"> <li>• Married</li> <li>• Unmarried</li> </ul>	63(43.67) 22(15.18)	49(31.01) 16(10.12)	6 2	2	$\chi^2$ Value:0.0317 Not significant
5	<b>Educational Qualification</b> <ul style="list-style-type: none"> <li>• Master Degree with B.Ed.,</li> <li>• Master Degree with M.Ed.,</li> <li>• Undergraduate with B.Ed.</li> </ul>	45(31.01%) 8 (5.69%) 32 (22.15%)	36(22.78%) 6 (3.79%) 23 (14.55%)	4 1 3	4	$\chi^2$ Value:0.1978 Not significant
6	<b>Teaching experience in number of years</b> <ul style="list-style-type: none"> <li>• &lt;10 Yrs</li> <li>• 10-20 Yrs</li> <li>• 20-30 Yrs</li> <li>• &gt;30 Yrs</li> </ul>	30 (20.88%) 46(31.01%) 7 (5.06%) 2 (1.89%)	23 (14.55%) 35 (22.15%) 6 (3.79%) 1 (0.63%)	3 3 1 1	6	$\chi^2$ Value:3.9707 Not significant
7	<b>Income</b> <ul style="list-style-type: none"> <li>• &lt;10000</li> <li>• 10001-20000</li> <li>• 20001-30000</li> <li>• &gt;30001</li> </ul>	34 (23.41%) 31 (20.88%) 13 (9.49%) 7 (5.06%)	27 (17.08%) 23 (14.55%) 10 (6.32%) 5 (3.16%)	3 2 2 1	6	$\chi^2$ Value:0.9607 Not significant
8	<b>Attended in-service education programme on Emotional and Behavioral Disorders of Children</b> <ul style="list-style-type: none"> <li>• Yes</li> <li>• No</li> </ul>	4 (3.79%) 81(55.6%)	3 (1.89%) 62 (39.24%)	2 6	2	$\chi^2$ Value:5.8461 Not significant
9	<b>Resident area</b> <ul style="list-style-type: none"> <li>• Urban</li> <li>• Rural</li> </ul>	50 (34.81%) 35 (24.05%)	38 (24.05%) 27 (17.08%)	5 3	2	$\chi^2$ Value:0.0481 Not significant
10	<b>Whom do you refer if the child has Emotional and Behavioral Disorders problems?</b> <ul style="list-style-type: none"> <li>• Psychiatrist</li> <li>• Psychologist</li> <li>• Child Specialist</li> </ul>	15 (10.12%) 23 (15.82%) 47 (32.91%)	11 (6.69%) 17 (10.75%) 37 (23.41%)	1 2 5	4	$\chi^2$ Value:0.2087 Not significant

#### 4.5 Section V- Effectiveness of Planned Teaching Programme On Pre-Test and Post-Test Knowledge Score

**TABLE NO. 5**  
**MEAN, SD, MEAN DIFFERENCE, 'T' VALUE OF PRETEST & POST-TEST KNOWLEDGE SCORES REGARDING**  
**EMOTIONAL AND BEHAVIORAL DISORDERS OF CHILDREN AMONG PRIMARY SCHOOL TEACHERS**  
**(N=158)**

Knowledge	Mean	SD	Mean Difference	df	't' Value
Pretest	8.60	±4.93	6.74	157	
Post-test	15.34	±4.70			

\*  $p < 0.05$

The data of table 5 depicted, that mean post-test knowledge score (15.34) is apparently higher than the mean pre-test knowledge score of (8.60). The dispersion of pretest scores ( $SD \pm 4.93$ ) is more than that of their post-test scores ( $SD \pm 4.70$ ) and the computed paired value shows that there is highly statistically significant difference between pre-test and post-test mean knowledge score ( $t_{(157)} = 13.80$ ,  $p < 0.05$  level). This indicates that planned teaching programme through planned teaching programme is effective in increasing knowledge score of Primary School Teachers regarding selected Emotional and Behavioral Disorders of children.

#### V. CONCLUSION

The main aim of the study was to evaluate the knowledge regarding the selected Emotional and Behavioral Disorder of children among Primary School Teachers. Planned teaching program was found as an effective method for information.

#### RECOMMENDATIONS

1. A similar study can be conducted by using true experimental design.
2. A study can be conducted to find out the factors that lead to selected Emotional and Behavioral Disorder of children.
3. A study can be conducted on parenting style to assess the selected Emotional and Behavioral Disorder of children.
4. A similar study can be done on a large sample.

#### REFERENCES

- [1]. Peate, I. L, Whiting. (2006). Caring for children and Families. England, John Wiley and Sons Ltd.
- [2]. Kothari, C. R. (2006). Research Methodology. New Delhi, New age International (P Ltd). Philadelphia, CV Mosby Company Published.
- [3]. Polit, D.F, Hangler. (1999). B.P Nursing Research, Principles and Methods. Philadelphia, J.B Lippincott Company.
- [4]. Singhal, P.K, (1991). Problem of Behaviour in Children. Delhi, CBS Publishers and Distributions.
- [5]. Sukhpal, Amarjeet Singh (2016). Simplified Nursing Research & Statistics for Undergraduates. CBS Publishers and Distributions Pvt. Ltd.

# Free-Radical Nonbranched-Chain Hydrogen Oxidation

Michael M. Silaev

Chemistry Faculty, Lomonosov Moscow State University, Vorobiev Gory, Moscow, 119991, Russia

**Abstract**— *New reaction scheme is suggested for the initiated nonbranched-chain addition of hydrogen atoms to the multiple bond of the molecular oxygen. The scheme includes the addition reaction of the hydroperoxyl free radical to the oxygen molecule to form the hydrotetraoxyl free radical which is relatively low-reactive and inhibits the chain process by shortening of the kinetic chain length. This reaction competes with chain propagation reactions through a hydrogen atom. Based on the proposed scheme rate equations (containing one to three parameters to be determined directly) are deduced using quasi-steady-state treatment. The kinetic description with use the obtained rate equations is applied to the  $\gamma$ -induced nonbranched-chain process of the free-radical oxidation of hydrogen dissolved in water containing different amounts of oxygen at 296 K. The ratio of rate constants of competing reactions and the rate constant of the addition reaction to the molecular oxygen are defined. In this process the oxygen with the increase of its concentration begins to act as an oxidation autoinhibitor (or an antioxidant), and the rate of hydrogen peroxide formation as a function of the dissolved oxygen concentration has a maximum. From the energetic standpoint possible nonchain pathways of the free-radical oxidation of hydrogen and the routes of ozone decay via the reaction with the hydroxyl free radical (including the addition yielding the hydrotetraoxyl free radical) in the Earth's upper atmosphere were considered.*

**Keywords**— *competition, hydrogen, low-reactive hydrotetraoxyl free radical, thermochemical data, energy.*

## I. INTRODUCTION

The kinetics of inhibition for nonbranched-chain processes of saturated free-radical addition to the C=C and C=O double bonds of alkene and formaldehyde molecules, respectively, by low-reactive free radicals that can experience delocalization of the unpaired  $p$ -electron was first considered in [1]. In these processes a low-reactive free radical is formed in the reaction competing with chain propagation reactions through a reactive free radical. In the present work the kinetics of inhibition by low-reactive hydrotetraoxyl free radical is considered for the nonbranched-chain process of the addition of a hydrogen atom to one of the two multiply bonded atoms of the oxygen molecule yielding a hydroperoxyl free radical. The hydroperoxyl free radical then abstracts the most labile atom from a molecule of the compound being oxidized or decomposes to turn into a molecule of an oxidation product. The only reaction that can compete with these two reactions at the chain evolution stage is the addition of the peroxy radical to the oxygen molecule (provided that the oxygen concentration is sufficiently high). This reaction yields the secondary hydrotetraoxyl 1:2 adduct radical, which is the heaviest and the largest among the reactants. It is less reactive than the primary peroxy 1:1 adduct radical and, as a consequence, does not participate in further chain propagation. At moderate temperatures, the reaction proceeds *via* a nonbranched-chain mechanism.

The aim of this study was the mathematical simulation of oxidation process autoinhibited by oxygen, when the dependence of the peroxide formation rate on the dissolved oxygen concentration has a maximum. The simulation was based on experimental data obtained for  $\gamma$ -radiation-induced addition reaction of hydrogen atom to the molecular oxygen for which the initiation rate  $V_1$  is known (taking into account that  $V = GP$  and  $V_1 = G(H^{\bullet})P$ , where  $P$  is the dose rate, and  $G(H^{\bullet})$  is the initial yield of the chain-carrier hydrogen atom  $H^{\bullet}$  – initiation yield [2, 3]).

Based on the reaction scheme suggested for the kinetic description of the addition process to oxygen, the kinetic equations with one to three parameters to be determined directly were derived. Reducing the number of unknown parameters in a kinetic equation will allow one to decrease the narrowness of the correlation of these parameters and to avoid a sharp buildup of the statistical error in the nonlinear estimation of these parameters in the case of a limited number of experimental data points. The rate constant of the addition to oxygen, estimated as a kinetic parameter, can be compared to its reference value if the latter is known. This provides a clear criterion to validate the mathematical description against experimental data.

## II. KINETICS OF HYDROGEN ATOM ADDITION TO THE OXYGEN MOLECULE

A number of experimental findings concerning the autoinhibiting effect of an increasing oxygen concentration at modest temperatures on hydrogen oxidation both in the gas phase [4–6] (Fig. 2) and in the liquid phase [7] (Fig. 1, curve 2),

considered in my earlier works [8–11], can also be explained in terms of the competition kinetics of free radical addition [12, 13]. From Fig. 2 shows that the quantum yields of hydrogen peroxide and water (of products of photochemical oxidation of hydrogen at atmospheric pressure and room temperature) are maximum in the region of small concentrations of oxygen in the hydrogen–oxygen system (curves 1 and 2, respectively) [4].

In the familiar monograph “Chain Reactions” by Semenov [14], it is noted that raising the oxygen concentration when it is already sufficient usually slows down the oxidation process by shortening the chains. The existence of the upper (second) ignition limit in oxidation is due to chain termination in the bulk through triple collisions between an active species of the chain reaction and two oxygen molecules (at sufficiently high oxygen partial pressures). In the gas phase at atmospheric pressure, the number of triple collisions is roughly estimated to be 103 times smaller than the number of binary collisions (and the probability of a reaction taking place depends on the specificity of the action of the third particle) [14]. Note that in the case of a gas-phase oxidation of hydrogen at low pressures of 25-77 Pa and a temperature of 77 K [5] when triple collisions are unlikely, the dependence of the rate of hydrogen peroxide formation on oxygen concentration (the rate of passing of molecular oxygen *via* the reaction tube) also has a pronounced maximum (see curves 3 and 4 in Fig. 2) that indicates a chemical mechanism providing the appearance of a maximum (see reaction 4 of *Scheme*).

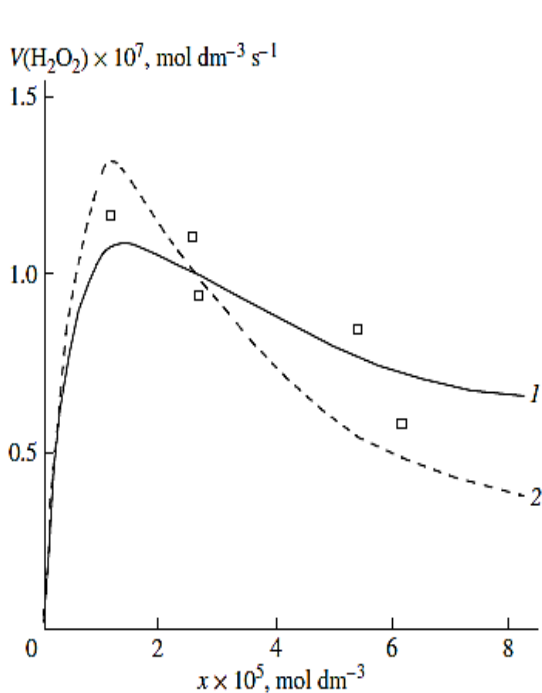


**FIGURE 1.** (1,  $\square$ ) Reconstruction of the functional dependence of the total hydrogen peroxide formation rate  $V_{3,7}(\text{H}_2\text{O}_2)$  on the dissolved oxygen concentration  $x$  from empirical data (symbols) using Eqs. (1a) and (4a) (model optimization with respect to the parameter  $\alpha$ ) for the  $\gamma$ -radiolysis of water saturated with hydrogen and containing different amounts of oxygen at 296 K [7] ( $S_Y = 1.13 \times 10^{-8}$ ).

(2) The dashed curve described  $V_3(\text{H}_2\text{O}_2)$  as a function of the oxygen concentration  $x$  based on Eq. (1a) (model optimization with respect to  $\alpha$ ) and the experimental data of curve 2 ( $S_Y = 1.73 \times 10^{-8}$ ).

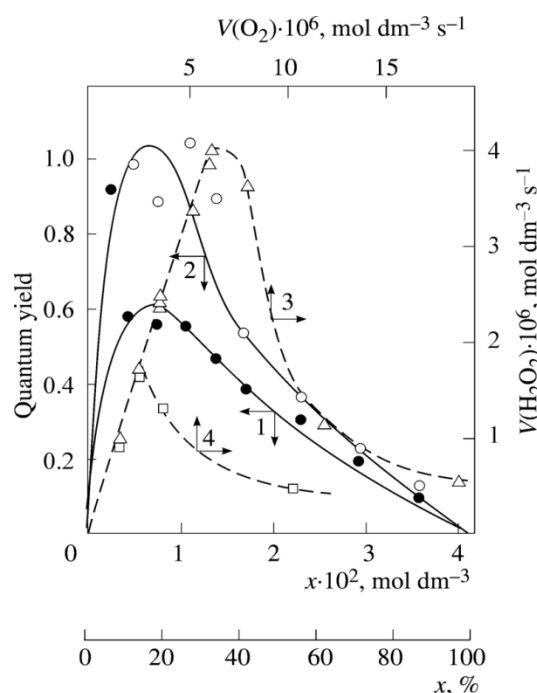
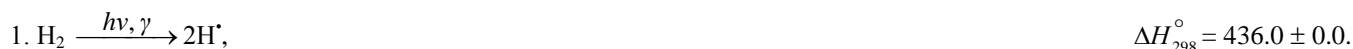


**FIGURE 2.** (1,  $\bullet$ ) Quantum yields of (1,  $\bullet$ ) hydrogen peroxide and (2,  $\circ$ ) water resulting from the photochemical oxidation of hydrogen in the hydrogen–oxygen system as a function of the oxygen concentration  $x$  (light wavelength of 171.9-172.5 nm, total pressure of  $10^5$  Pa, room temperature [4]). (3, 4) Hydrogen peroxide formation rate  $V(\text{H}_2\text{O}_2)$  (dashed curves) as a function of the rate  $V(\text{O}_2)$  at which molecular oxygen is passed through a gas-discharge tube filled with (3,  $\triangle$ ) atomic and (4,  $\square$ ) molecular hydrogen. Atomic hydrogen was obtained from molecular hydrogen in the gas-discharge tube before the measurements (total pressure of 25-77 Pa, temperature of 77 K [5]). The symbols represent experimental data.

### III. SCHEME

Nonbranched-chain oxidation of hydrogen and changes in enthalpy ( $\Delta H_{298}^{\circ}$ , kJ mol<sup>-1</sup>) for elementary reactions<sup>1</sup>

#### Chain initiation



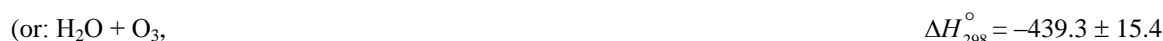
#### Chain propagation



#### Inhibition



#### Chain termination



The chain evolution (propagation and inhibition) stage of the *Scheme* includes consecutive reaction pairs 2–3 and 3–3'; the parallel (competing) reaction pair 3–4; and consecutive–parallel reactions 2 and 4.

The hydroperoxyl free radical  $\text{HO}_2^{\bullet}$  [23–26] resulting from reaction 2 possesses an increased energy due to the energy released the conversion of the O=O multiple bond into the HO–O' ordinary bond. Therefore, before its possible decomposition, it can interact with a hydrogen or oxygen molecule as the third body *via* parallel (competing) reactions 3 and 4, respectively. The hydroxyl radical  $\text{HO}^{\bullet}$  that appears and disappears in consecutive parallel reactions 3 (first variant) and 3' possesses additional energy owing to the exothermicity of the first variant of reaction 3, whose heat is distributed between the two products. As a consequence, this radical has a sufficiently high reactivity not to accumulate in the system during these reactions, whose rates are equal ( $V_3 = V_{3'}$ ) under quasi-steady-state conditions, according to the above scheme. Parallel reactions 3 (second, parenthesized variant) and 3' regenerate hydrogen atoms. It is assumed [9, 10] that the hydrotetraoxyl radical  $\text{HO}_4^{\bullet}$  (first reported in [27–29]) resulting from endothermic reaction 4, which is responsible for the peak in the

<sup>1</sup>According to Francisco and Williams [15], the enthalpy of formation ( $\Delta H_f^{\circ}$ ) in the gas phase of  $\text{H}^{\bullet}$ ,  $\text{HO}^{\bullet}$ ,  $\text{HO}_2^{\bullet}$ ,  $\text{HO}_4^{\bullet}$  (the latter without the possible intramolecular hydrogen bond taken into account),  $\text{O}_3$ ,  $\text{H}_2\text{O}$  [6],  $\text{H}_2\text{O}_2$ , and  $\text{H}_2\text{O}_4$  is  $218.0 \pm 0.0$ ,  $39.0 \pm 1.2$ ,  $12.6 \pm 1.7$ ,  $122.6 \pm 13.7$ ,  $143.1 \pm 1.7$ ,  $-241.8 \pm 0.0$ ,  $-136.0 \pm 0$ , and  $-26.0 \pm 9$  kJ mol<sup>-1</sup>, respectively. Calculations for the  $\text{HO}_4^{\bullet}$  radical with a helical structure were carried out using the G2(MP2) method [16]. The stabilization energies of  $\text{HO}_2^{\bullet}$ ,  $\text{HO}_4^{\bullet}$ , and  $\text{HO}_3^{\bullet}$  were calculated in the same work to be  $64.5 \pm 0.1$ ,  $69.5 \pm 0.8$ , and  $88.5 \pm 0.8$  kJ mol<sup>-1</sup>, respectively. The types of the  $\text{O}_4$  molecular dimers, their IR spectra, and higher oxygen oligomers were reported [17, 18]. The structure and IR spectrum of the hypothetical cyclotetraoxygen molecule  $\text{O}_4$ , a species with a high energy density, were calculated by the CCSD method, and its enthalpy of formation was estimated [19]. The photochemical properties of  $\text{O}_4$  and the van der Waals nature of the  $\text{O}_2$ – $\text{O}_2$  bond were investigated [20, 21]. The most stable geometry of the dimer is two  $\text{O}_2$  molecules parallel to one another. The  $\text{O}_4$  molecule was identified by NR mass spectrometry [22].

experimental rate curve (Fig. 2, curve 3), is closed into a five-membered  $[\overline{\text{OO}-\text{H}\cdots\text{OO}}]'$  cycle due to weak intramolecular hydrogen bonding [30, 31]. This structure imparts additional stability to this radical and makes it least reactive.

The  $\text{HO}_4^\bullet$  radical was discovered by Staehelin *et al.* [32] in a pulsed radiolysis study of ozone degradation in water; its UV spectrum with an absorption maximum at 260 nm ( $\epsilon(\text{HO}_4^\bullet)_{260\text{nm}} = 320 \pm 15 \text{ m}^2 \text{ mol}^{-1}$ ) was reported. The spectrum of the  $\text{HO}_4^\bullet$  radical is similar to that of ozone, but the molar absorption coefficient  $\epsilon(\text{HO}_4^\bullet)_{\lambda_{\text{max}}}$  of the former is almost two times larger [32]. The assumption about the cyclic structure of the  $\text{HO}_4^\bullet$  radical can stem from the fact that its mean lifetime in water at 294 K, which is  $(3.6 \pm 0.4) \times 10^{-5}$  s (as estimated [11] from the value of  $1/k$  for the monomolecular decay reaction  $\text{HO}_4^\bullet \xrightarrow{k} \text{HO}_2^\bullet + \text{O}_2$  [32]), is 3.9 times longer than that of the linear  $\text{HO}_3^\bullet$  radical [16, 33] estimated in the same way [11] for the same conditions [34],  $(9.1 \pm 0.9) \times 10^{-6}$  s.

MP2/6-311++G\*\* calculations using the Gaussian-98 program confirmed that the cyclic structure of  $\text{HO}_4^\bullet$  [35] is energetically more favorable than the helical structure [16] (the difference in energy is 4.8–7.3 kJ mol<sup>-1</sup>, depending on the computational method and the basis set).<sup>2</sup> For example, with the MP2(full)/6-31G(d) method, the difference between the full energies of the cyclic and acyclic  $\text{HO}_4^\bullet$  conformers with their zero-point energies (ZPE) values taken into account (which reduces the energy difference by 1.1 kJ mol<sup>-1</sup>) is -5.1 kJ mol<sup>-1</sup> and the entropy of the acyclic-to-cyclic  $\text{HO}_4^\bullet$  transition is  $\Delta S_{298}^\circ = -1.6 \text{ kJ mol}^{-1} \text{ K}^{-1}$ . Therefore, under standard conditions,  $\text{HO}_4^\bullet$  can exist in both forms, but the cyclic structure is obviously dominant (87%,  $K_{\text{eq}} = 6.5$ ) [35].

Reaction 4 and, to a much lesser degree, reaction 6 inhibit the chain process, because they lead to inefficient consumption of its main participants –  $\text{HO}_2^\bullet$  and  $\text{H}^\bullet$ .

The hydrogen molecule that results from reaction 5 in the gas bulk possesses an excess energy, and, to acquire stability within the approximation used in this work, it should have time for deactivation *via* collision with a particle M capable of accepting the excess energy [37]. To simplify the form of the kinetic equations, it was assumed that the rate of the bimolecular deactivation of the molecule substantially exceeds the rate of its monomolecular decomposition, which is the reverse of reaction 5 [38].

Reactions<sup>3</sup> 6 and 7 regenerate hydrogen and oxygen (in the form of  $\text{O}_2(X^3\Sigma_g^-)$  molecules, including the singlet states with  $\Delta H_{f298}^\circ(\text{O}_2, a^1\Delta_g) = 94.3 \text{ kJ mol}^{-1}$  [15, 18] and  $\Delta H_{f298}^\circ(\text{O}_2, b^1\Sigma_g^+) = 161.4 \text{ kJ mol}^{-1}$  [18], which are deactivated by collisions, and in the form of  $\text{O}_3$ ) and yield hydrogen peroxide or water *via* a nonchain mechanism, presumably through the intermediate formation of the unstable hydrogen tetraoxide molecule  $\text{H}_2\text{O}_4$  [39, 40].<sup>4</sup> Ozone does not interact with molecular hydrogen. At moderate temperatures, it decomposes fairly slowly, particularly in the presence of  $\text{O}_2(X^3\Sigma_g^-)$  [18]. The reaction of ozone with  $\text{H}^\bullet$  atoms, which is not impossible, results in their replacement with  $\text{HO}^\bullet$  radicals. The relative

<sup>2</sup>There were calculations for the two conformers (*cis* and *trans*) of the  $\text{HO}_4^\bullet$  radical [36] using large scale *ab initio* methods and density functional techniques with extended basis sets. Both conformers have a nearly planar geometry with respect to the four oxygen atoms and present an unusually long central O–O bond. The most stable conformer of  $\text{HO}_4^\bullet$  radical is the *cis* one, which is computed to be endothermic with respect to  $\text{HO}_2^\bullet(X^2A'') + \text{O}_2(X^3\Sigma_g^-)$  at 0 K.

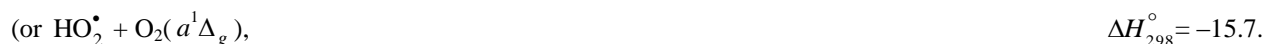
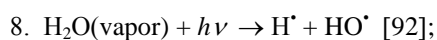
<sup>3</sup>Taking into account the principle of detailed balance for the various pathways of formation of products, whose numbers in the elementary reaction should not exceed three for possible involvement in the triple collisions in the case of the reverse reaction, since the probability of simultaneous interaction of four particles is negligible.

<sup>4</sup>The planar, six-atom, cyclic, hydrogen-bonded dimer  $(\text{HO}_2)_2$  was calculated using quantum chemical methods (B3LYP density functional theory) [88]. The hydrogen bond energy is 47.7 and 49.4 kJ mol<sup>-1</sup> at 298 K for the triplet and singlet states of the dimer, respectively.

contributions from reactions 6 and 7 to the process kinetics can be roughly estimated from the corresponding enthalpy increments (*Scheme*).

When there is no excess hydrogen in the hydrogen–oxygen system, the homomolecular dimer  $O_4$  [19–22, 41, 42], which exists at low concentrations (depending on the pressure and temperature) in equilibrium with  $O_2$  [18], can directly capture the  $H^\bullet$  atom to yield the heteronuclear cluster<sup>5</sup>  $HO_4^\bullet$ . This  $HO_4^\bullet$  cluster is more stable than  $O_4$  [18] and cannot abstract a hydrogen atom from the hydrogen molecule. Therefore, in this case, nonchain hydrogen oxidation will occur to give molecular oxidation products *via* the disproportionation of free radicals.

The low-reactive hydrotetraoxyl radical  $HO_4^\bullet$  [32], which presumably has a high energy density [19], may be an intermediate in the efficient absorption and conversion of biologically hazardous UV radiation energy the Earth upper atmosphere. The potential energy surface for the atmospheric reaction  $HO^\bullet + O_3$ , in which the adduct  $HO_4^\bullet(2A)$  was considered as an intermediate, was calculated by the DMBE method [43]. From this standpoint, the following reactions are possible in the upper troposphere, as well as in the lower and middle stratosphere, where most of the ozone layer is situated (altitude of 16–30 km, temperature of 217–227 K, pressure of  $1.0 \times 10^4 - 1.2 \times 10^3$  Pa [44]; the corresponding  $\Delta H_{298}^\circ$  reaction values are given in  $\text{kJ mol}^{-1}$  [15]):



The  $HO_4^\bullet$  radical can disappear *via* disproportionation with a molecule, free radical, or atom in addition to dissociation. Note that emission from  $O_2(a^1\Delta_g)$  and  $O_2(b^1\Sigma_g^+)$  is observed at altitudes of 30–80 and 40–130 km, respectively [45].

Staehelin *et al.* [32] pointed out that, in natural systems in which the concentrations of intermediates are often very low, kinetic chains in chain reactions can be very long in the absence of scavengers since the rates of the chain termination reactions decrease with decreasing concentrations of the intermediates according to a quadratic law, whereas the rates of the chain propagation reactions decrease according to a linear law.

The kinetic description of the noncatalytic oxidation of hydrogen, including in an inert medium [37], in terms of the simplified scheme of free-radical nonbranched-chain reactions (*Scheme*), which considers only quadratic-law chain termination and ignores the surface effects [5], at moderate temperatures and pressures, in the absence of transitions to unsteady-state critical regimes, and at a substantial excess of the hydrogen concentration over the oxygen concentration was obtained by means of quasi-steady-state treatment, as in the previous studies on the kinetics of the branched-chain free-radical oxidation of hydrogen [46], even though the applicability of this method in the latter case under unsteady states conditions was insufficiently substantiated. The method was used with the following condition<sup>6</sup> for the first stages of the process:  $k_6 = \sqrt{2k_5 2k_7}$  [47] and, hence,  $V_1 = V_5 + 2V_6 + V_7 = (\sqrt{2k_5} [H^\bullet] + \sqrt{2k_7} [HO_4^\bullet])^2$  which allow the exponent of the  $2k_5[H^\bullet]^2$  term in the  $d[H^\bullet]/dt = 0$  equation to be reduced to 1 [1, 47]. The kinetic equations were derived for the rates ( $\text{mol dm}^{-3} \text{ s}^{-1}$ ) of the elementary reactions for the formation of molecular products of hydrogen oxidation.

The kinetic equations were derived for the rates ( $\text{mol dm}^{-3} \text{ s}^{-1}$ ) of the elementary reactions for the formation of molecular products of hydrogen oxidation.

The rate of the chain formation of hydrogen peroxide in propagation reaction 3 and of water in reactions 3 and 3' with  $V_{3,3'}(\text{H}_2\text{O}) = 2V_3$  is

<sup>5</sup>It is impossible to make a sharp distinction between the two-step bimolecular interaction of three species *via* the equilibrium formation of the labile intermediate  $O_4$  and the elementary trimolecular reaction  $O_2 + O_2 + H^\bullet \rightarrow HO_4^\bullet$ .

<sup>6</sup>For example, the ratio of the rate constants of the bimolecular disproportionation and dimerization of free radicals at room temperature is  $k(\text{HO}^\bullet + \text{HO}_2^\bullet)/[2k(2\text{HO}^\bullet)2k(2\text{HO}_2^\bullet)]0.5 = 2.8$  in the atmosphere [44] and  $k(\text{H}^\bullet + \text{HO}^\bullet)/[2k(2\text{H}^\bullet)2k(2\text{HO}^\bullet)]0.5 = 1.5$  in water [3]. These values that are fairly close to unity.

$$V_3(\text{H}_2\text{O}_2; \text{H}_2\text{O}) = V_3(\text{H}_2\text{O}) = V_1 \alpha l k_2 x / f \quad (1)$$

$$= V_1 \alpha l x / f_m \quad (1a)$$

In this equation<sup>7</sup>,  $V_1$  is the initiation rate,  $l = [\text{H}_2]$  and  $x = [\text{O}_2]$  are the molar concentrations of the reactants with  $l \gg x$ ;  $\alpha = k_3/k_4$  is the ratio of the rate constants of the competing (parallel) reactions;  $k_2 = \alpha l_m \sqrt{2k_5 V_1} / x_m^2$  is the rate constant of reaction 2 of hydrogen atom addition to the oxygen molecule, whose analytical expression is obtained by the solution to the quadratic equation derived from the condition of the extremum of the rate function  $\partial V_3 / \partial x = 0$ ;  $l_m$  and  $x_m$  are the concentrations of the components  $l$  and  $x$ , respectively, at the maximum of the function;  $f = k_2 x^2 + (\alpha l + x) \sqrt{2k_5 V_1}$  and  $f_m = x^2 + (\alpha l + x) x_m^2 / \alpha l_m$ ; and  $2k_5$  is the rate constant of hydrogen atom recombination reaction 5 considered to be bimolecular in this approximation.

The rate constant  $2k_5$  in the case of the pulsed radiolysis of ammonia–oxygen (+ argon) gaseous mixtures at a total pressure of  $10^5$  Pa and a temperature of 349 K was calculated to be  $1.6 \times 10^8 \text{ dm}^3 \text{ mol}^{-1} \text{ s}^{-1}$  [6] (a similar value of this constant for the gas phase was reported in an earlier publication [48]). Pagsberg *et al.* [6] found that the dependence of the yield of the intermediate  $\text{HO}^\bullet$  on the oxygen concentration has a maximum close to  $5 \times 10^{-4} \text{ mol dm}^{-3}$ . In the computer simulation of the process, they considered the strongly exothermic reaction  $\text{HO}_2^\bullet + \text{NH}_3 \rightarrow \text{H}_2\text{O} + \text{NHOH}$ , which is similar to reaction 3 in *Scheme*, whereas the competing reaction 4 was not taken into account.

The ratio of the rates of the competing reactions is  $V_3/V_4 = \alpha l/x$  and the chain length is  $\nu = V_3/V_1$ . Equation (1a) was obtained by substitution of the rate constant  $k_2$  into Eq. (1) with its analytical expression (in order to reduce the number of unknown parameters that are to be measured directly). The optimum concentration  $x_m$  of oxygen, at which the rate of oxidation is maximum, can be calculated from Eq. (1a) or the analytical expression for  $k_2$  if other parameters that appear in these expressions are known.

The rates of nonchain formation of molecular hydrogen, hydrogen peroxide, and water in reactions 5, 6, and 7 of quadratic chain termination are as follows:

$$V_5 = V_1^2 2k_5 (\alpha l + x)^2 / f^2, \quad (2)$$

$$2V_6 = 2V_1 \sqrt{2k_5 V_1} (\alpha l + \beta + x) k_2 x^2 / f^2, \quad (3)$$

$$V_7 = V_1 (k_2 x^2)^2 / f^2. \quad (4)$$

The designations of the parameters in this equation are the same as in Eq. (1).

The rate of the nonbranched-chain free-radical oxidation of hydrogen is a complex function of the rates of formation and disappearance of  $\text{H}^\bullet$  atoms and  $\text{HO}_4^\bullet$  radicals:  $V_1 + V_{3,3'} - V_4 - V_5 + V_7$ . Unlike the dependences of the rates  $V_4$  ( $V_4 \leq V_1$ ),  $V_5$ , and  $V_7$ , the dependences of the rates  $V_2$ ,  $V_{3,3'}$ , and  $2V_6$  on the oxygen concentration  $x$  show a maximum.

Equation (1) under the conditions (a)  $k_2 x^2 \ll (\alpha l + x) \sqrt{2k_5 V_1}$ ,  $\alpha l \gg x$  and (b)  $k_2 x^2 \gg (\alpha l + x) \sqrt{2k_5 V_1}$ , corresponding to the ascending and descending branches of the curve with a maximum, can be transformed into simple equations which allow preliminary to estimate the parameters  $\alpha$  and  $k_2$  and express directly and inversely proportional functions of concentration  $x$ :

$$V_3 = \sqrt{V_1} k_2 x / \sqrt{2k_5}, \quad (5)$$

$$V_3 = V_1 \alpha l / \varphi x, \quad (6)$$

<sup>7</sup>This equation can be used to describe a wide range of nonbranched-chain reactions of addition of any free radicals to the C=C bonds of unsaturated hydrocarbons, alcohols, etc., which result in the formation of molecular 1:1 adducts in binary reaction systems of saturated and unsaturated components [1, 9, 10].

where  $\varphi = 2$  at maximum when  $k_2x^2 \cong (\alpha l + x)$  and  $\varphi = 1$  at the decreasing part of the curve.

In the case of nonchain hydrogen oxidation *via* the above addition reaction ( $H^\bullet + O_4 \xrightarrow{k_{add}} HO_4^\bullet$ ), the formation rates of the molecular oxidation products in reactions 6 and 7 (*Scheme*,  $k_2 = k_3 = k_4 = 0$ ) are defined by modified Eqs. (3) and (4) in which  $\beta = 0$ ,  $(\alpha l + x)$  is replaced with 1, and  $k_2$  is replaced with  $k_{add}K_{eq}$  ( $k_{add}K_{eq}$  is the effective rate constant of  $H^\bullet$  addition to the  $O_4$  dimer,  $K_{eq} = k/k'$  is the equilibrium constant of the reversible reaction  $2O_2 \xrightleftharpoons[k']{k} O_4$  with  $k' \gg k_{add}[H^\bullet]$ ). The formation rates of the stable products of nonchain oxidation ( $k_3 = 0$ ), provided that either reactions 2 and 4 or reaction 2 alone ( $k_4 = 0$ ) occurs (*Scheme*; in the latter case, reactions 6 and 7 involve the  $HO_2^\bullet$  radical rather than  $HO_4^\bullet$ ), are given by modified Eqs. (3) and (4), in which  $(\alpha l + x)$  replaced with 1, and  $x^2$  replaced with  $x$ . In the latter case, the  $HO_2^\bullet$  radical, rather than  $HO_4^\bullet$ , takes part in reactions 6 and 7.

It is important to note that, if in the *Scheme* chain initiation *via* reaction 1 is due to the interaction between molecular hydrogen and molecular oxygen yielding the hydroxyl radical  $HO^\bullet$  instead of  $H^\bullet$  atoms and if this radical reacts with an oxygen molecule (reaction 4) to form the hydrotrioxyl radical  $HO_3^\bullet$  (which was obtained in the gas phase by neutralization reionization (NR) mass spectrometry [33] and has a lifetime of  $>10^{-6}$  s at 298 K) and chain termination takes place *via* reactions 5–7 involving the  $HO^\bullet$  and  $HO_3^\bullet$ , radicals instead of  $H^\bullet$  and  $HO_4^\bullet$ , respectively, the expression for the water chain formation rates (the chain formation of hydrogen peroxide in this kinetic model does not occur) derived in the same way will appear as a fractional rational function of the oxygen concentration  $x$  without a maximum:  $V_3(H_2O) = V_3(H_2O) = V_1k_3l/(k_4x + \sqrt{2k_5V_1})$ .

Curve 2 in Fig. 1 describes, in terms of the overall equation  $V_{3,7} = V_1x(\alpha f_m + x^3)/f_m^2$  for the rates of reactions 3 and 7 (which was derived from Eqs. (1a) and (4), respectively, at that Eq. (4) in the form [49] of  $V_7 = V_1x^4/f_m^2$  (4a) in which  $k_2$  is replaced with its analytical expression  $\alpha l_m \sqrt{2k_5V_1}/x_m^2$  derived from Eq. (1)), the dependence of the hydrogen peroxide formation rate (minus the rate  $V_{H_2O_2} = 5.19 \times 10^{-8}$  mol dm<sup>-3</sup> s<sup>-1</sup> of the primary formation of hydrogen peroxide after completion of the reactions in spurs) on the concentration of dissolved oxygen during the  $\gamma$ -radiolysis of water saturated with hydrogen (at the initial concentration  $7 \times 10^{-4}$  mol dm<sup>-3</sup>) at 296 K [7]. These data were calculated in the present work from the initial slopes of hydrogen peroxide buildup versus dose curves for a <sup>60</sup>Co  $\gamma$ -radiation dose rate of  $P = 0.67$  Gy s<sup>-1</sup> and absorbed doses of  $D \cong 22.5$ –304.0 Gy. The following values of the primary radiation-chemical yield  $G$  (species per 100 eV of energy absorbed) for water  $\gamma$ -radiolysis products in the bulk of solution at pH 4–9 and room temperature were used (taking into account that  $V = GP$  and  $V_1 = G_H P$ ):  $G_{H_2O_2} = 0.75$  and  $G_H = 0.6$  (initiation yield) [3];  $V_1 = 4.15 \times 10^{-8}$  mol dm<sup>-3</sup> s<sup>-1</sup>;  $2k_5 = 2.0 \times 10^{10}$  dm<sup>3</sup> mol<sup>-1</sup> s<sup>-1</sup> [3]. As can be seen from Fig. 1, the best description of the data with an increase in the oxygen concentration in water is attained when the rate  $V_7$  of the formation of hydrogen peroxide *via* the nonchain mechanism in the chain termination reaction 7 (curve 1,  $\alpha = (8.5 \pm 2) \times 10^{-2}$ ) is taken into account in addition to the rate  $V_3$  of the chain formation of this product *via* the propagation reaction 3 (dashed curve 2,  $\alpha = 0.11 \pm 0.026$ ). The rate constant of addition reaction 2 determined from  $\alpha$  is substantially underestimated:  $k_2 = 1.34 \times 10^7$  (vs.  $2.0 \times 10^{10}$  [3]) dm<sup>3</sup> mol<sup>-1</sup> s<sup>-1</sup>. The difference can be due to the fact that the radiation-chemical specifics of the process were not considered in the kinetic description of the experimental data. These include oxygen consumption *via* reactions that are not involved in the hydrogen oxidation *Scheme* and reverse reactions resulting in the decomposition of hydrogen peroxide by intermediate products of water radiolysis ( $e_{aq}^-$ ,  $H^\bullet$ ,  $HO^\bullet$ ), with the major role played by the hydrated electron [3].

#### IV. CONCLUSIONS

Thus, the addition reaction of the  $HO_2^\bullet$  radical that possesses an elevated energy *in statu nascendi* with the oxygen molecule (at sufficiently high oxygen concentrations) to give the  $HO_4^\bullet$  radical was used for the first time in the kinetic description of the initiated hydrogen oxidation at moderate temperature and pressure [9, 10]. This reaction is endothermic and competes

with the chain propagation reaction *via* the H<sup>•</sup> atom. The HO<sub>4</sub><sup>•</sup> radical generated in the former reaction has a low reactivity and inhibits the chain reaction.<sup>8</sup>

The above data concerning the competition kinetics of the nonbranched-chain addition of hydrogen atoms to the multiple bonds of the oxygen molecules make it possible to describe, using rate equations (1a) and (4a), obtained by quasi-steady-state treatment, the peaking experimental dependences of the formation rates of molecular 1:1 adduct H<sub>2</sub>O<sub>2</sub> on the concentration of the oxygen over the entire range of its variation in binary system (Fig. 1). In such reaction systems consisting of saturated and unsaturated components [51, 52], the unsaturated compound (in this case the O<sub>2</sub>) is both a reactant and an autoinhibitor, specifically, a source of low-reactive free radicals (in this case the HO<sub>4</sub><sup>•</sup> radicals) shortening kinetic chains.

The progressive inhibition of the nonbranched-chain processes, which takes place as the concentration of the unsaturated compound is raised (after the maximum process rate is reached), can be an element of the self-regulation of the natural processes that returns them to the stable steady state.

Using mechanism of the nonbranched-chain free-radical hydrogen oxidation considered here, it has been demonstrated that, in the Earth's upper atmosphere, the decomposition of O<sub>3</sub> in its reaction with the HO<sup>•</sup> radical can occur *via* the addition of the latter to the ozone molecule, yielding the HO<sub>4</sub><sup>•</sup> radical, which is capable of efficiently absorbing UV radiation [32].

## REFERENCES

- [1] M. M. Silaev and L. T. Bugaenko, "Mathematical Simulation of the Kinetics of Radiation Induced Hydroxyalkylation of Aliphatic Saturated Alcohols", *Radiation Physics and Chemistry*, 1992, vol. 40, no. 1, pp. 1–10.
- [2] M. M. Silaev, "Applied Aspects of the  $\gamma$ -Radiolysis of C<sub>1</sub>–C<sub>4</sub> Alcohols and Binary Mixtures on Their Basis", *Khimiya Vysokikh Energii*, Vol. 36, No. 2, 2002, pp. 97–101, English Translation in: *High Energy Chemistry*, 2002, vol. 36, no. 2, pp. 70–74.
- [3] A. K. Pikaev, "Sovremennaya radiatsionnaya khimiya. Radioliz gazov i zhidkosti" ("Modern Radiation Chemistry: Radiolysis of Gases and Liquids"), Nauka, Moscow, 1986.
- [4] H. A. Smith and A. Napravnik, "Photochemical Oxidation of Hydrogen", *Journal of the American Chemistry Society*, 1940, vol. 62, no. 1, pp. 385–393.
- [5] E. J. Badin, "The Reaction between Atomic Hydrogen and Molecular Oxygen at Low Pressures. Surface Effects", *Journal of the American Chemistry Society*, 1948, vol. 70, no. 11, pp. 3651–3655.
- [6] P. B. Pagsberg, J. Eriksen, and H. C. Christensen, "Pulse Radiolysis of Gaseous Ammonia–Oxygen Mixtures", *The Journal of Physical Chemistry*, 1979, vol. 83, no. 5, pp. 582–590.
- [7] N. F. Barr and A. O. Allen, "Hydrogen Atoms in the Radiolysis of Water", *The Journal of Physical Chemistry*, 1959, vol. 63, no. 6, pp. 928–931.
- [8] M. M. Silaev, "A New Competitive Kinetic Model of Radical Chain Oxidation: Oxygen as an Autoinhibitor", *Biofizika*, 2001, vol. 46, no. 2, pp. 203–209, English Translation in: *Biophysics*, 2001, vol. 46, no. 2, pp. 202–207.
- [9] M. M. Silaev, "The Competition Kinetics of Nonbranched Chain Processes of Free-Radical Addition to Double Bonds of Molecules with the Formation of 1:1 Adducts and the Inhibition by the Substrate", *Oxidation Communication*, 1999, vol. 22, no. 2, pp. 159–170.
- [10] M. M. Silaev, "The Competition Kinetics of Radical-Chain Addition", *Zhurnal Fizicheskoi Khimii*, Vol. 73, No. 7, 1999, pp. 1180–1184, English Translation in: *Russian Journal of Physical Chemistry*, 1999, vol. 73, no. 7, pp. 1050–1054.
- [11] M. M. Silaev, "Competitive Mechanism of the Nonbranched Radical Chain Oxidation of Hydrogen Involving the Free Cyclohydrotetraoxyl Radical [OO<sup>•</sup>–H<sup>•</sup>–OO<sup>•</sup>], which Inhibits the Chain Process", *Khimiya Vysokikh Energii*, 2003, vol. 37, no. 1, pp. 27–32, English Translation in: *High Energy Chemistry*, 2003, vol. 37, no. 1, pp. 24–28.
- [12] M. M. Silaev, "Simulation of the Initiated Addition of Hydrocarbon Free Radicals and Hydrogen Atoms to Oxygen *via* a Nonbranched Chain Mechanism", *Teoreticheskie Osnovy Khimicheskoi Tekhnologii*, 2007, vol. 41, no. 6, pp. 634–642, English Translation in: *Theoretical Foundation of Chemical Engineering*, 2007, vol. 41, no. 6, pp. 831–838.
- [13] M. M. Silaev, "Simulation of Initiated Nonbranched Chain Oxidation of Hydrogen: Oxygen as an Autoinhibitor", *Khimiya Vysokikh Energii*, 2008, vol. 42, no. 2, pp. 124–129, English Translation in: *High Energy Chemistry*, 2008, vol. 42, no. 1, pp. 95–100.
- [14] N. N. Semenov, "Tsepnye reaktsii" ("Chain Reactions"), Goskhimtekhnizdat, Leningrad, 1934, pp. 241, 203.
- [15] J. S. Francisco and I. H. Williams, "The Thermochemistry of Polyoxides and Polyoxy Radicals", *International Journal of Chemical Kinetics*, 1988, vol. 20, no. 6, pp. 455–466.

<sup>8</sup>Note that in the case of similar nonbranched-chain (i.e., "slow") oxidation of RH hydrocarbons, the corresponding reactive RO<sub>2</sub><sup>•</sup> and low-reactive RO<sub>4</sub><sup>•</sup> radicals participate in the process [50]. The only difference between the kinetic model of oxidation and the kinetic model of the chain addition of 1-hydroxyalkyl radicals to the free (unsolvated) form of formaldehyde in nonmethanolic alcohol–formaldehyde systems [1, 9, 10] is that in the former does not include the formation of the molecular 1:1 adduct *via* reaction 4.

- [16] D. J. McKay and J. S. Wright, "How Long Can You Make an Oxygen Chain?", *Journal of the American Chemistry Society*, 1998, vol. 120, no. 5, pp. 1003–1013.
- [17] N. P. Lipikhin, "Dimers, Clusters, and Cluster Ions of Oxygen in the Gas Phase", *Uspekhi Khimii*, 1975, vol. 44, no. 8, pp. 366–376.
- [18] S. D. Razumovskii, "Kislorod – elementarnye formy i svoistva" ("Oxygen: Elementary Forms and Properties"), Khimiya, Moscow, 1979.
- [19] K. M. Dunn, G. E. Scuceria, and H. F. Schaefer III, "The infrared spectrum of cyclotetraoxygen, O<sub>4</sub>: a theoretical investigation employing the single and double excitation coupled cluster method", *The Journal of Chemical Physics*, 1990, vol. 92, no. 10, pp. 6077–6080.
- [20] L. Brown and V. Vaida, "Photoreactivity of Oxygen Dimers in the Ultraviolet", *The Journal of Physical Chemistry*, 1996, vol. 100, no. 19, pp. 7849–7853.
- [21] V. Aquilanti, D. Ascenzi, M. Bartolomei, D. Cappelletti, S. Cavalli, M. de Castro-Vitores, and F. Pirani, "Molecular Beam Scattering of Aligned Oxygen Molecules. The Nature of the Bond in the O<sub>2</sub>–O<sub>2</sub> Dimer", *Journal of the American Chemistry Society*, 1999, vol. 121, no. 46, pp. 10794–1080.
- [22] F. Cacace, G. de Petris, and A. Troiani, "Experimental Detection of Tetraoxygen", *Angewandte Chemie, International Edition* (in English), 2001, vol. 40, no. 21, pp. 4062–4065.
- [23] H. S. Taylor, "Photosensitisation and the Mechanism of Chemical Reactions", *Transactions of the Faraday Society*, 1926, vol. 21, no. 63(3), pp. 560–568.
- [24] S. N. Foner and R. L. Hudson, "Mass spectrometry of the HO<sub>2</sub> free radical", *The Journal of Chemical Physics*, 1962, vol. 36, no. 10, p. 2681.
- [25] S. N. Foner and R. L. Hudson, "Mass spectrometry of the HO<sub>2</sub> free radical", *The Journal of Chemical Physics*, 1962, vol. 36, no. 10, p. 2681.
- [26] P. D. Lightfoot, B. Veyret, and R. Lesclaux, "Flash Photolysis Study of the CH<sub>3</sub>O<sub>2</sub> + HO<sub>2</sub> Reaction between 248 and 573 K", *The Journal of Physical Chemistry*, 1990, vol. 94, no. 2, pp. 708–714.
- [27] P. Smith, "The HO<sub>3</sub> and HO<sub>4</sub> Free Radicals", *Chemistry and Industry*, 1954, no. 42, pp. 1299–1300.
- [28] A. J. B. Robertson, "A Mass Spectral Search for H<sub>2</sub>O<sub>4</sub> and HO<sub>4</sub> in a Gaseous Mixture Containing HO<sub>2</sub> and O<sub>2</sub>", *Chemistry and Industry*, 1954, no. 48, p. 1485.
- [29] D. Bahnmann and E. J. Hart, "Rate Constants of the Reaction of the Hydrated Electron and Hydroxyl Radical with Ozone in Aqueous Solution", *The Journal of Physical Chemistry*, 1982, vol. 86, no. 2, pp. 252–255.
- [30] G. C. Pimentel and A. L. McClellan, "The Hydrogen Bond", L. Pauling, Editor, Freeman, San Francisco, 1960, p. 200.
- [31] "Vodorodnaya svyaz": Sbornik statei" ("The Hydrogen Bonding: Collection of Articles") N. D. Sokolov, Editor, Nauka, Moscow, 1981.
- [32] J. Staehelin, R. E. Bühler, and J. Hoigné, "Ozone Decomposition in Water Studied by Pulse Radiolysis. 2. OH and HO<sub>4</sub> as Chain Intermediates", *The Journal of Physical Chemistry*, 1984, vol. 88, no. 24, pp. 5999–6004.
- [33] F. Cacace, G. de Petris, F. Pepi, and A. Troiani, "Experimental Detection of Hydrogen Trioxide", *Science*, 1999, vol. 285, no. 5424, pp. 81–82.
- [34] R. F. Bühler, J. Staehelin, and J. Hoigné, "Ozone Decomposition in Water Studied by Pulse Radiolysis. 1. HO<sub>2</sub>/O<sub>2</sub><sup>-</sup> and HO<sub>3</sub>/O<sub>3</sub><sup>-</sup> as Intermediates", *The Journal of Physical Chemistry*, 1984, vol. 88, no. 12, pp. 2560–2564.
- [35] I. V. Trushkov, M. M. Silaev, and N. D. Chuvylkin, "Acyclic and Cyclic Forms of the Radicals HO<sub>4</sub><sup>•</sup>, CH<sub>3</sub>O<sub>4</sub><sup>•</sup>, and C<sub>2</sub>H<sub>5</sub>O<sub>4</sub><sup>•</sup>: Ab Initio Quantum Chemical Calculations", *Izvestiya Akademii Nauk, Ser.: Khimiya*, 2009, no. 3, pp. 479–482, English Translation in: *Russian Chemical Bulletin, International Edition*, 2009, vol. 58, no. 3, pp. 489–492.
- [36] A. Mansergas, J. M. Anglada, S. Olivella, M. F. Ruiz-López, "On the Nature of the Unusually Long OO Bond in HO<sub>3</sub> and HO<sub>4</sub> Radicals", *Phys. Chem. Chem. Phys.*, 2007, vol. 9, no. 44, pp. 5865–5873.
- [37] W. Wong and D. D. Davis, "A Flash Photolysis Resonance Fluorescence Study of the Reactions of Atomic Hydrogen and Molecular Oxygen: H + O<sub>2</sub> + M → HO<sub>2</sub> + M", *International Journal of Chemical Kinetics*, 1974, vol. 6, no. 3, pp. 401–416.
- [38] S. W. Benson, "Thermochemical Kinetics: Methods for the Estimation of Thermochemical Data and Rate Parameters", 2nd Edition, Wiley, New York, 1976.
- [39] Yagodovskaya, T.V. and Nekrasov, L.I., "Use of Infrared Spectroscopy to Study Frozen Hydrogen–Oxygen Systems Containing Hydrogen Polyoxides", *Zhurnal Fizicheskoi Khimii*, 1977, vol. 51, no. 10, pp. 2434–2445.
- [40] X. Xu, R. P. Muller, and W. A. Goddard III, "The Gas Phase Reaction of Singlet Dioxygen with Water: a Water-Catalyzed Mechanism", *Proceedings of the National Academy Sciences of the United States of America*, 2002, vol. 99, no. 6, pp. 3376–3381.
- [41] E. T. Seidl and H. F. Schaefer III, "Is There a Transition State for the Unimolecular Dissociation of Cyclotetraoxygen (O<sub>4</sub>)?", *The Journal of Chemical Physics*, 1992, vol. 96, no. 2, pp. 1176–1182.
- [42] R. Hernández-Lamonedá and A. Ramírez-Solís, "Reactivity and Electronic States of O<sub>4</sub> along Minimum Energy Paths", *The Journal of Chemical Physics*, 2000, vol. 113, no. 10, pp. 4139–4145.
- [43] A. J. C. Varandas and L. Zhang, "Test Studies on the Potential Energy Surface and Rate Constant for the OH + O<sub>3</sub> Atmospheric Reaction", *Chemical Physics Letters*, 2000, vol. 331, nos. 5–6, pp. 474–482.
- [44] "Atmosfera. Spravochnik" ("Atmosphere: A Handbook"), Gidrometeoizdat, Leningrad, 1991.
- [45] H. Okabe, "Photochemistry of Small Molecules", Wiley, New York, 1978.

- [46] A. B. Nalbandyan and V. V. Voevodskii, "Mekhanizm okisleniya i goreniya vodoroda" ("Mechanism of Hydrogen Oxidation and Combustion"), V. N. Kondrat'ev, Editor, Akad. Nauk SSSR, Moscow, 1949.
- [47] L. Bateman, "Olefin Oxidation", Quarterly Reviews, 1954, vol. 8, no. 2, pp. 147–167.
- [48] A. W. Boyd, C. Willis, and O. A. Miller, "A Re-examination of the Yields in the High Dose Rate Radiolysis of Gaseous Ammonia", Canadian Journal of Chemistry, 1971, vol. 49, no. 13, pp. 2283–2289.
- [49] M. M. Silaev, "Competition Mechanism of Substrate-Inhibited Radical Chain Addition to Double Bond", Neftekhimiya, 2000, vol. 40, no. 1, pp. 33–40, English Translation in: Petroleum Chemistry, 2000, vol. 40, no. 1, pp. 29–35.
- [50] M. Silaev, Mathematical Simulation of Kinetics of Radiation-Induced Free-Radical Oxidation by Nonbranched-Chain Mechanism // *Recent Innovations in Chemical Engineering*, 2015, vol. 8, no. 2, pp. 112–124.
- [51] M. M. Silaev, "Low-reactive Free Radicals Inhibiting Nonbranched Chain Processes of Addition", *Biofizika*, 2005, vol. 50, no. 4, pp. 585–600, English Translation in: *Biophysics*, 2005, vol. 50, no. 4, pp. 511–524.
- [52] M. M. Silaev, Kinetics of the Free-Radical Nonbranched-Chain Addition // *American Journal of Polymer Science and Technology*, 2017, vol. 3, no. 3, pp. 29-49.

# Zig-zag theories differently accounting for layerwise effects of multilayered composites

Andrea Urraci<sup>1</sup>, Ugo Icardi<sup>2</sup>

Dipartimento di Ingegneria Meccanica e Aerospaziale, Politecnico di Torino, Italy

**Abstract**—This paper essays the effects of the choice of through-thickness representation of variables and of zig-zag functions within a general theory by the authors from which the theories considered are particularized. Characteristic feature, coefficients are calculated using symbolic calculus, so to enable an arbitrary choice of the representation. Such choice and that of zig-zag functions is shown to be always immaterial whenever coefficients are recalculated across the thickness by enforcing the fulfillment of elasticity theory constraints. Assigning a specific role to each coefficient is shown immaterial. Moreover, the order of representation of displacements can be freely exchanged with one another and, most important, zig-zag functions can be omitted if part of coefficients are calculated enforcing the interfacial stress field compatibility. Vice versa, accuracy of theories that only partially satisfy constraints, is shown to be strongly dependent upon the assumptions made. Applications to laminated and soft-core sandwich plates and beams having different length-to-thickness ratios, different material properties and thickness of constituent layers, various boundary conditions and distributed or localized loading are presented. Solutions are found in analytic form assuming the same trial functions and expansion order for all theories. Numerical results show which simplifications are yet accurate and therefore admissible.

**Keywords**—Composite and sandwich plates, zig-zag theories, interlaminar transverse shear/normal stress continuity, localized and distributed loadings, FEA 3-D elastostatic solutions.

## I. INTRODUCTION

Laminated and sandwich composites, which find continuously increasing applications because of their superior specific strength and stiffness, better energy absorption, fatigue properties and corrosion resistance than traditional materials, need to be analyzed with specific structural models.

Indeed, differently from non-layered materials their displacement field can no longer be  $C^1$ -continuous, but instead has to be  $C^0$ -continuous, i.e. slope discontinuities must occur at the interfaces of layers with different properties as only in this way local equilibrium equations can be satisfied, which means that out-of-plane shear and normal stresses and the transverse normal stress gradient must be continuous at interfaces (zig-zag effect).

As a result of the strong differences between in-plane and transversal properties, 3-D stress fields arise whose out-of-plane components can assume the same importance as those in the plane and which play a fundamental role in the formation and growth mechanisms of damage and for failure. Considered that multilayer composites are used for the construction of primary structures, this being the only way to fully exploit their advantages, so far many multilayered theories of various order and degree have been developed, wherein sandwiches are described as multilayered structures whenever cell scale effect of honeycomb core aren't the object of the analysis. Sandwiches are often described as three-layer laminates where the core is assumed as the intermediate layer being shear resistant in the transverse direction, free of in-plane normal and shear stresses and deformable in the thickness direction (see, e.g. Frostig and Thomsen [1]). But often higher-order sandwich theories are considered wherein in-plane and transverse displacements vary nonlinearly across the thickness, taking different forms in the faces and the core (see, Rao and Desai [2] and Yang et al. [3]), or a separate representation is used for each of them (see, Cho et al. [4]).

A broad discussion of this matter is found, among many others, in the papers by Carrera and co-workers [5-9], Demasi [10], Vasilive and Lur'e [11], Reddy and Robbins [12], Lur'e, and Shumova [13], Noor et al. [14], Altenbach [15], Khandan et al. [16] and Kapuria and Nath [17] and the book by Reddy [18]. As shown by the quoted contributions, theories can be categorized into equivalent single-layer (ESL) formulations borrowed from those for isotropic materials, which completely disregard layerwise effects and therefore they are only suitable for predicting overall response quantities (but not even for all loading, material properties and stack-up and certainly not for sandwiches as shown e.g. [19] to [25]) and layerwise formulations which differently account for layerwise and zig-zag effects, presenting a different degree of accuracy in predicting through-thickness displacement and stress fields and a different computational burden. Layerwise theories further

subdivide into discrete-layer (DL) and zig-zag (ZZ) theories (acronyms used throughout the paper are defined in Table 1), the former assuming a representation apart for each layer having its own d.o.f., which could overwhelm the computational capacity when structures of industrial interest are analyzed but that is still always accurate irrespective for lay-up, layer properties, loading and boundary conditions considered, the latter incorporating layewise functions into a global representation.

**TABLE 1**  
**Acronyms; in bold the new theories; <sup>(n)</sup> degree of displacements**

Acronym	Description(section)	Acronym	Description(section)
FEA-3D	Mixed solid finite elements [31].	MHWZZA4	Mixed HW theory [25].
HRZZ	Mixed HR theory, $u_{\alpha,\beta}^{(3)}$ , $u_{\zeta}^{(0)}$ , [25].	ZZA	$u_{\alpha,\beta}^{(3)}$ , $u_{\zeta}^{(4)}$ [23] (2.3).
HRZZ4	Mixed HR theory, $u_{\alpha,\beta}^{(3)}$ , $u_{\zeta}^{(4)}$ , [25]	ZZA*	$u_{\alpha,\beta}^{(3)}$ , $u_{\zeta}^{(4)}$ [24] (2.4).
HSDT_34	Enriched adaptive versions of HSDT $u_{\alpha,\beta}^{(3)}$ , $u_{\zeta}^{(4)}$ (2.6).	ZZA*_43	$u_{\alpha,\beta}^{(4)}$ , $u_{\zeta}^{(3)}$ (2.6).
HWZZ	HW mixed version of ZZA [25] (2.5).	<b>ZZA*_43PRM</b>	$u_{\alpha,\beta}^{(4)}$ , $u_{\zeta}^{(3)}$ (2.6).
HWZZ_RDF	Modified HWZZ theory (2.6).	ZZA_RDF	Modified ZZA theory (2.3).
HWZZM	HWZZ with different zig-zag functions [24] (2.7).	ZZA-XX	Zig-zag general theory with exponential representation (3).
HWZZM*	HWZZ with different zig-zag functions [24] (2.7).	ZZA-XX'	Zig-zag general theory with power representation (3).
MHR	Mixed HR theory with Murakami's zig-zag function for $u_{\alpha,\beta}^{(3)}$ , ( $u_{\zeta}^{(4)}$ lacking), [25]	ZZA_X1 ZZA_X2 ZZA_X3 ZZA_X4	$u_{\alpha,\beta}^{(3)}$ , $u_{\zeta}^{(4)}$ (3).
MHR4	Mixed HR theory, displacements with Murakami's zig-zag function [25].	<b>ZZA_X1*</b> <b>ZZA_X2*</b> <b>ZZA_X3*</b> <b>ZZA_X4*</b>	$u_{\alpha,\beta}^{(3)}$ , $u_{\zeta}^{(4)}$ (3).
MHWZZA	Mixed HW theory [25].		

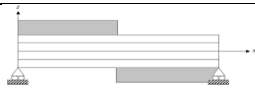
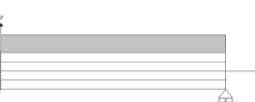
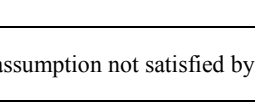
ZZ subdivide in turn into displacement-based and mixed theories, as strains and stresses could be chosen separately from one another using mixed variational theorems, and into physically-based (DZZ) and kinematic-based (MZZ) theories, since layerwise contributions are expressed differently. Regardless of this, ZZ have anyway intermediate features between ESL and DL that allow them to strike the right balance between accuracy and cost saving and so to meet designers' demand of theories in a simple already accurate form. Layerwise contributions are embodied in DZZ as the product of linear [26] or nonlinear [27] zig-zag functions and unknown zig-zag amplitudes, while they are a priori assumed to feature a periodic change of the slope of displacements at interfaces in MZZ, as it happens for periodic lay-ups but applying it in any case, consequently they are referred as kinematic-based theories. Stresses being assumed apart from kinematics, MZZ constitute mixed theories that because their layerwise functions are insensitive to the physical characteristics of the lamination and their kinematics is simplified in general accurately describe through-thickness stress fields but not always as accurately displacements [23-25]. Generally but still not always, because mixed formulations are also known as discussed in [25], stresses of DZZ derive from kinematics which, having to adequately represent them through strain-displacement relations, has to be rather complex so to a priori satisfy interfacial stress compatibility conditions (hence DZZ generally constitute physically-based theories), provides through-thickness displacement fields that are adequately reproduced even at interfaces where the slope doesn't reverse and so MZZ fail.

Carrera Unified Formulation (CUF) [6], which to date is extensively used to carry out analyses of multi-layered structures, as it allows displacements to take arbitrary forms that can be chosen by the user as an input and therefore allows to study general loading and boundary conditions, can be ascribed as a first approximation in the field of MZZ theories since no

physical constraints are enforced to define layerwise functions and it gets existing ESL and MZZ as particularizations. However also refined DZZ [23-25] have shown a comparable degree of generality and flexibility of use compared to CUF, resulting even more efficient because they allow the same accuracy with fewer variables. According to this, the last generation of DZZ with coefficients redefined across each physical or computational lamina must be tested for many other challenging cases similar to those already studied by researchers who used CUF and it is also necessary to check whether further generalizations can be produced as these DZZ have a computational burden still comparable to that of ESL and therefore less than that of the CUF and the DL, at least for the cases so far explored. As shown in [25], DZZ with five fixed d.o.f. can be developed and successfully applied to the analysis of challenging benchmarks with a through-thickness variable kinematic representation able to satisfy all constraints by the elasticity theory, which can be arbitrarily chosen by the user so that accurate theories can be derived with feature similar to those of CUF and HT theories with a hierarchical set of locally defined polynomials (see, Catapano et al. [28] and de Miguel et al. [29]), which neither incorporate zig-zag contributions nor require post-processing steps, but instead require a larger number of degrees of freedom and a larger expansion order of analytical solutions. As also shown in [25], advanced forms of DZZ can be developed considering forms of representation different for each displacement with zig-zag functions completely different from those usually considered until now, or even omitting them without any accuracy loss, provided that a sufficient number of coefficients is enforced which can be redefined across the thickness through the enforcement of physical constraints, therefore in a way to some extent similar to global-local superposition theories by Zhen and Wanji, e.g. [30].

Further research is required to get even whether these findings hold in general for arbitrary lay-ups, loading and boundary conditions and material properties of constituent layers. To contribute to this matter, in this paper theories developed by the authors in [23-25] are retaken and new ones obtained assuming differently the representation of displacement components are considered. They are applied to a number of challenging cases whose lay-up, material properties of layers, dimensions, boundary conditions, normalizations, trial functions and expansion order used to find analytical solutions are reported in Tables 2a and 2b, while mechanical properties of are reported in Table 2c. The results of theories for the challenging elastostatic cases with strong layerwise effects considered, which comprise localized loading and clamped edges, are compared each other and to exact solutions and to 3-D FEA [31] results, in order to show on a broader series of theories and benchmarks than in [25] that whenever the expressions of coefficients of displacements are determined a priori by enforcing the fulfillment of the full set of interfacial stress compatibility conditions, of stress boundary conditions, as well as local equilibrium equations at a number of selected point sufficient to determine all coefficients, the choice of the representation and of zig-zag functions can be arbitrary without the results changing. Under these conditions it will be proven that those zig-zag functions can even be omitted, with self-evident advantages from the computational standpoint. The numerical results also aim to demonstrate that when only a partial set of conditions is satisfied, vice versa the accuracy of theories returns to depend heavily on the type of representation and on zig-zag functions chosen.

**TABLE 2a**  
**Geometry, loading and boundary conditions**

Case	Layer thickness	Material	Sketch	Loading	Lx/h
a (§)	[0.1h/0.4h]s	[Gr-Ep / Foam / Gr-Ep]		$p^0(x) = p_u^0 \sin(2\pi x / L_x)$ if $0 \leq x \leq L_x$	10
b (*§)	[0.1h/0.4h]s	[Gr-Ep / Foam / Gr-Ep]		$p^0(x) = \begin{cases} p_u^0 & \text{if } 0 \leq x \leq L_x/2 \\ -p_u^0 & \text{if } L_x/2 \leq x \leq L_x \end{cases}$	10
c (*§)	[0.1h/0.4h]s	[Gr-Ep / Foam / Gr-Ep]		$p^0(x) = p_u^0$ if $0 \leq x \leq L_x$	14.286
d (*§)	[(2h/7) / (4h/7) / (h/7) ]	[n/n/n]		$p^0(x) = p_u^0$ if $0 \leq x \leq L_x$	5.714
e (§)	[(2h/7) / (4h/7) / (h/7) ]	[n/n/n]			
Murakami's function assumption not satisfied by $u_\alpha$ (*), $u_\beta$ (□) or $u_\zeta$ (§)					

**TABLE 2b**  
**Trial functions, expansion order and normalizations.**

Case	Trial functions	Expansion	Normalization
a	$u^0(x, y) = \sum_{m=1}^M A_m \cos\left(\frac{2m\pi x}{L_x}\right);$ $w^0(x, y) = \sum_{m=1}^M C_m \sin\left(\frac{2m\pi x}{L_x}\right);$ $\gamma_x^0(x, y) = \sum_{m=1}^M D_m \cos\left(\frac{2m\pi x}{L_x}\right);$	1	$\bar{u} = \frac{u(0, z)}{hp^0} \quad \bar{w} = \frac{w\left(\frac{L_x}{4}, z\right)}{hp^0}$ $\bar{\sigma}_{xx} = \frac{\sigma_{xx}\left(\frac{L_x}{4}, z\right)}{p^0(L_x/h)^2} \quad \bar{\sigma}_{xz} = \frac{\sigma_{xz}(0, z)}{p^0} \quad \bar{\sigma}_{zz} = \frac{\sigma_{zz}\left(\frac{L_x}{4}, z\right)}{p^0}$
b		1	
c		1	
d	$u^0(x, y) = \sum_{i=1}^I A_i \left(\frac{x}{L}\right)^i;$ $w^0(x, y) = \sum_{i=1}^I C_i \left(\frac{x}{L}\right)^i;$	9	$\bar{u} = \frac{u(L_x, z)}{hp^0} \quad \bar{w} = \frac{w(L_x, z)}{hp^0}$ $\bar{\sigma}_{xx} = \frac{\sigma_{xx}(L_x, z)}{p^0(L_x/h)^2} \quad \bar{\sigma}_{xz} = \frac{A\sigma_{xz}(L_x, z)}{P^0 L_x} \quad \bar{\sigma}_{zz} = \frac{\sigma_{zz}(L_x, z)}{p^0}$
e	$\gamma_x^0(x, y) = \sum_{i=1}^I D_i \left(\frac{x}{L}\right)^i$	9	$\bar{u} = \frac{u(L_x, z)}{hp^0} \quad \bar{w} = \frac{w(L_x, z)}{hp^0}$ $\bar{\sigma}_{xx} = \frac{\sigma_{xx}(L_x, z)}{p^0(L_x/h)^2} \quad \bar{\sigma}_{xz} = \frac{\sigma_{xz}(L_x, z)}{P^0} \quad \bar{\sigma}_{zz} = \frac{\sigma_{zz}(L_x, z)}{p^0}$

**TABLE 2c**  
**Mechanical properties of constituent layers.**

Material name	E1[GPa]	E2[GPa]	E3[GPa]	G12 [GPa]	G13 [GPa]	G23 [GPa]	v12	v13	v23
Foam	0.035	0.035	0.035	0.0123	0.0123	0.0123	0.4	0.4	0.4
Gr-Ep	132.38	10.76	10.76	5.65	5.65	3.61	0.24	0.24	0.49
n [iso]	-	-	M1	-	-	-	0.33	0.33	0.33

M1  $E_u/E_l=1.6, E_u/E_c=166.6 \cdot 10^5;$  [iso]=isotropic  $E_1=E_2=E_3 \quad G_1=G_2=G_3$

**II. THEORETICAL FRAMEWORK**

The feature of zig-zag theories retaken from [23] to [25] and those of new ones proposed in this paper are discussed below, but just displacement, and only for mixed formations also strain and stress fields, will be discussed since governing equations as well as any intermediate step can be obtained in a straightforward way using standard techniques. As in [23] to [25] a symbolic calculus tool is used, which allows to get closed form expressions of coefficients as a result of the enforcement of physical constraints once and for all and which allows the user to arbitrarily choose the form of representation, the rest being automatic. For clarity, first the notations and the basic assumptions used (common for all the theories) are defined, then theories are examined.

**2.1 Notations and basic assumptions**

Layers are assumed to be linear elastic, with a uniform thickness  $h^k$  and to be perfectly bonded to each other (bonding resin interlayer disregarded). According, sandwiches are described in homogenized form as multi-layered structures with a thick soft intermediate layer as the core. A Cartesian coordinate reference system  $(x, y, z)$  is assumed as the reference frame,  $(x, y)$  being on the middle reference plane  $\Omega$ , so  $z$  being the thickness coordinate, and the overall thickness of the laminate is indicated by  $h$ .  $L_x$  and  $L_y$  symbolize the plate side-length in the  $x$ - and  $y$ -directions. Symbols  $^{(k)}z^+$  and  $^{(k)}z^-$  are assumed to represent the thickness coordinates just passed or just below the interface  $k$ , respectively. Subscripts  $_k$  and superscripts  $^k$  chosen as appropriate indicate that quantities belong to the layer  $k$ , while  $^u$  and  $^l$  indicate upper and lower faces of the laminate. In-plane and transverse components of elastic displacements are indicated as  $u_\alpha$  and  $u_\zeta$ . Strains, assumed to be infinitesimal, and stresses are symbolized by  $\varepsilon_{ij}$  and  $\sigma_{ij}$ , respectively. A comma is used to indicate spatial derivatives (e.g.,  $(\cdot)_{,x} = \partial/\partial x, (\cdot)_{,z} = \partial/\partial z$ ). The middle-plane displacements  $u^0, v^0, w^0$  and the rotations of the normal  $\theta_\alpha$  (summing shear rotation  $\Gamma_\alpha^0$  and flexural notation  $-w^0(\alpha, \beta)_{,\alpha}$ ) are assumed as the only degrees of freedom for each theory. To be concise, symbols  $x, y, z$  can be replaced through the paper by Greek letters (e.g.  $\alpha = 1, 2 \equiv x, y; \zeta = 3 \equiv z$ ).

Note that throughout this paper the appellation of higher-order theories is reserved to ZZA [23], ZZA\*, HWZZM, HWZZM\* retaken from [24], HWZZ [25], HSDT\_34, ZZA\*\_43, ZZA-XX, ZZA-XX', ZZA\_RDF, HWZZ\_RDF and ZZA\_X1 to \_X4 retaken from an article completed just before the present one and submitted for publication to another journal and ZZA\*\_43PRM, ZZA\_X1\* to X4\* introduced in this paper. The appellation lower-order is attributed to theories HRZZ, HRZZ4, MHWZZA, MHWZZA4, MHR and MHR4 from [25]. It is reminded that acronyms and basic features of all theories considered in this paper are explained in Table 1.

## 2.2 Methodology of solution

Solutions are searched in analytical form as a truncated series expansion of unknown amplitudes  $A_{\Delta}^i$  and trial functions  $\mathfrak{R}^i(x, y)$  that individually satisfy the prescribed boundary conditions, which is symbolized as:

$$\Delta = \sum_{i=1}^{m_{\Delta}} A_{\Delta}^i \mathfrak{R}^i(x, y) \quad (1)$$

Here  $\Delta$  symbolises in turns the d.o.f.  $u^0$ ,  $v^0$ ,  $w^0$ ,  $\theta_{\alpha}$ . The candidate solution (1) is substituted into the Principle of Virtual Work, or within mixed variational functional and the solution is found using Raileigh-Ritz's like and Lagrange multipliers methods. Namely,  $\mathfrak{R}^i(x, y)$  are chosen to satisfy geometric boundary conditions, while mechanical boundary conditions are satisfied using Lagrange multipliers method. A number of unknown amplitudes are determined in this latter way, according to the type and number of conditions for each specific case, while the remaining ones are determined deriving the above mentioned functionals with respect to each amplitude  $A_{\Delta}^i$  and equating to zero. Table 2b reports the expressions of  $\mathfrak{R}^i(x, y)$  for each specific case, along with the expansion order used. The same representation and the same order of expansion are shared by all theories for each examined problem, to carry out comparisons under the same conditions.

Discontinuous loading distributions considered in the numerical applications are studied without using a series expansion with a very large number of components because the symbolic calculus tool used to construct theories allows to represent loading as a general function  $\chi(x, y)$  acting on upper and/or lower faces, or just on a part of them, whose relative energy contribution is computed exactly, so that the structural model is simplified and at the same time made more accurate.

The following boundary conditions are enforced on the reference mid-surface at the clamped edge of propped-cantilever beams, herein assumed at  $x=0$ :

$$u^0(0,0) = 0; w^0(0,0) = 0; w^0(0,0)_{,x} = 0; \Gamma_x^0(0,0) = 0 \quad (2)$$

In order to simulate that (2) holds identically across the thickness, the following further boundary conditions are enforced:

$$u_{\alpha}(0, z)_{,z} = 0; u_{\zeta}(0, z)_{,z} = 0; u_{\zeta}(0, z)_{,xz} = 0 \quad (3)$$

To ensure that the transverse shear stress resultant force equals the constraint force, it should be also enforced the following mechanical boundary condition

$$\int_{-h/2}^{h/2} \sigma_{xz}(0, z) dz = T \quad (4)$$

The additional support condition  $w^0(L, -h/2) = 0$  holds at  $x=L$  on the lower face  $z = -h/2$ , while condition (4) is reformulated as:

$$\int_{-h/2}^{h/2} \sigma_{xz}(L, z) dz = T_L \quad (4')$$

As mentioned above, the latter mechanical boundary conditions are enforced using Lagrange multipliers method. At simply-supported edges, the following boundary conditions are enforced on the reference mid-plane:

$$\begin{aligned} w^0(0, y) = 0; w^0(L, y) = 0; w^0(0, y)_{,xx} = 0; w^0(L, y)_{,xx} = 0 \\ w^0(x, 0) = 0; w^0(x, L_y) = 0; w^0(x, 0)_{,yy} = 0; w^0(x, L_y)_{,yy} = 0 \end{aligned} \quad (5)$$

The constraints being assumed to act at  $x=0$ ,  $x=L_x$  and  $y=0$ ,  $y=L_y$  ( $L_x, L_y$  being the length of sides parallel to  $x$ ,  $y$  axes). In the applications, plates in cylindrical bending are considered, square or rectangular plates having been already extensively studied in [24],[25]. The boundary conditions for cylindrical bending follows in a straightforward way from (5) assuming that no variations occur in the  $y$ , so that  $(x, z)$  is the plane where bending take place.

### 2.3 ZZA displacement-based theory

This zig-zag theory, developed in [23], applied in [24, 25] and from which other theories of this paper are particularized or constitute a generalization, postulates the following displacement field across the thickness:

$$\begin{aligned} u_\alpha(x, y, z) &= [ u^0(x, y) + z(\Gamma_\alpha^0(x, y) - w^0(x, y)_{,\alpha}) ]_0 + [ F_\alpha^u(z) ]_i + [ \sum_{k=1}^{n_i} \Phi_\alpha^k(x, y)(z - z_k) H_k(z) + \sum_{k=1}^{n_\alpha} C_u^k(x, y) H_k(z) ]_c \\ u_\zeta(x, y, z) &= [ w^0(x, y) ]_0 + [ F_\zeta^c(z) ]_i + [ \sum_{k=1}^{n_i} \Psi^k(x, y)(z - z_k) H_k(z) + \sum_{k=1}^{n_\zeta} \Omega^k(x, y)(z - z_k)^2 H_k(z) + \sum_{k=1}^{n_\zeta} C_\zeta^k(x, y) H_k(z) ]_c \end{aligned} \quad (6)$$

Summing up, the linear contribution  $[...]_0$  incorporates and introduces only the d.o.f. of the theory and has coefficients already all defined, while higher-  $[...]_i$  and layerwise  $[...]_c$  contributions contain coefficients whose expressions have to be determined in terms of the d.o.f., of their derivatives, of geometric and of material properties by enforcing the fulfillment of stress boundary conditions

$$\sigma_{\alpha\zeta} = \sigma_{\zeta\zeta,\zeta} = 0; \sigma_{\zeta\zeta} = p^0(\pm) \quad (7)$$

at upper (+) and lower (-) laminate bounding faces,  $p^0(\pm)$  being the transverse distributed loading acting on these faces, as well as the enforcement of local equilibrium equations:

$$\sigma_{\alpha\beta,\beta} + \sigma_{\alpha\zeta,\zeta} = b_\alpha \quad ; \quad \sigma_{\alpha\zeta,\alpha} + \sigma_{\zeta\zeta,\zeta} = b_\zeta \quad (8)$$

at selected points across the thickness and of stress-compatibility equations at material layer interfaces

$$\begin{aligned} \sigma_{\alpha\zeta}^{(k)z^+} &= \sigma_{\alpha\zeta}^{(k)z^-}; \sigma_{\zeta\zeta}^{(k)z^+} = \sigma_{\zeta\zeta}^{(k)z^-}; \\ \sigma_{\zeta\zeta,\zeta}^{(k)z^+} &= \sigma_{\zeta\zeta,\zeta}^{(k)z^-} \end{aligned} \quad (9)$$

In details, any combination of independent functions  $[ F_\alpha^u(z) ]_i$  and  $[ F_\zeta^c(z) ]_i$  of any degree can be chosen

$$\begin{aligned} [ F_\alpha^u(z) ]_i &= [ C_\alpha^i(x, y)z^2 + D_\alpha^i(x, y)z^3 + (Oz^4 \dots) ]_i = [ {}_3(\tilde{\gamma}_\alpha) ]_i + [ (Oz^4 \dots) ]_i \\ [ F_\zeta^c(z) ]_i &= [ b^i(x, y)z + c^i(x, y)z^2 + d^i(x, y)z^3 + e^i(x, y)z^4 + (Oz^5 \dots) ]_i = [ {}_4(\tilde{\gamma}_\zeta) ]_i + [ (Oz^5 \dots) ]_i \end{aligned} \quad (10)$$

Since coefficients of contributions  $Oz^4 \dots$  and  $Oz^5 \dots$  can be always determined by enforcing (8) in a suited number of points selected across the thickness. In this way, a variable kinematics representation is allowed that enables ZZA to adapt to changes in solutions across the thickness, which is worth the name of “adaptive” theory given to this theory. Instead, the expressions of coefficients  $C_\alpha^i$ ,  $D_\alpha^i$ ,  $b^i$  to  $e^i$  are determined by enforcing the fulfillment of stress boundary conditions (7), while those of  $\Phi_\alpha^k$ ,  $\Psi^k$  and  $\Omega^k$  are determined so that the continuity (9) of out-of-plane stresses and of the transverse normal stress gradient  $\sigma_{\zeta\zeta,\zeta}$  at layer interfaces are met. The remaining layerwise contributions  $C_u^k$  and  $C_\zeta^k$  are determined restoring the continuity of displacements

$$u_\alpha^{(k)z^+} = u_\alpha^{(k)z^-}; u_\zeta^{(k)z^+} = u_\zeta^{(k)z^-} \quad (11)$$

at mathematical layer interfaces whenever the expressions of  $[ F_\alpha^u(z) ]_i$  and  $[ F_\zeta^c(z) ]_i$  change. The readers can find all the details herein omitted for brevity in [23-25]. It is worth mentioning that SEUPT technique [23] can be used in order to obtain a  $C^0$  formulation of the ZZA theory, as well as of all the other theories of this paper which follow.

A variant of ZZA, called ZZA\_RDF and retaken from a paper recently submitted for publication is here reported, whose coefficients assumes a different role than ZZA. Particularly,  $\Omega^k$ ,  $\Psi^k$ ,  $\Phi_\alpha^k$  impose the fulfillment of local equilibrium equations at different points across the thickness (for  $i>1$ , where I is the number of computational layer) while  $C_\alpha^i$ ,  $d^i$  and  $e^i$  impose the continuity of out-of-plane stresses at the interfaces between layers. Because of some laminations, stresses could be erroneously predicted to vanish for  $z=0$ , a different reference plane with a distance far  $h_d > h/2$  from the bottom face is assumed:

$$\begin{aligned} u_\alpha(x, y, z) &= [ u^0(x, y) + (z - h_d + h/2)(\Gamma_\alpha^0(x, y) - w^0(x, y)_{,\alpha}) ]_0 + [ C_\alpha^i(x, y)z^2 + D_\alpha^i(x, y)z^3 ]_i + [ \sum_{k=1}^{n_i} \Phi_\alpha^k(x, y)(z - z_k)H_k(z) + \sum_{k=1}^{n_i} C_u^k(x, y)H_k(z) ]_c \\ u_z(x, y, z) &= [ w^0(x, y) ]_0 + [ b^i(x, y)z + c^i(x, y)z^2 + d^i(x, y)z^3 + e^i(x, y)z^4 ]_i + [ \sum_{k=1}^{n_i} \Psi^k(x, y)(z - z_k)H_k(z) + \sum_{k=1}^{n_i} \Omega^k(x, y)(z - z_k)^2 H_k(z) + \sum_{k=1}^{n_i} C_\zeta^k(x, y)H_k(z) ]_c \\ &(h_d \leq z \leq h_d + h) \end{aligned} \quad (11')$$

Results of this theory are indistinguishable from those of ZZA in the present numerical applications. As a consequence, it will be demonstrated that is not necessary to assign a specific role to coefficients if the full set of physical constraints is imposed and coefficients are redefined layer-by-layer across the thickness.

#### 2.4 ZZA\* displacement-based theory

This theory, which is the first developed by the authors [24] to prove that constraints (9) can be enforced without explicitly incorporating zig-zag functions and relative amplitudes  $\Phi_\alpha^k$ ,  $\Psi^k$  and  $\Omega^k$  inside  $[...]_c$  and from which other theories follow as generalizations in this paper, has the following displacement field:

$$\begin{aligned} u_\alpha(x, y, z) &= [ u^0(x, y) + z(\Gamma_\alpha^0(x, y) - w^0(x, y)_{,\alpha}) ]_0 + \left\{ \sum_{k=1}^{n_i} {}_k \tilde{B}_\alpha^i(x, y)z + [C_\alpha^i(x, y)z^2] + [D_\alpha^i(x, y)z^3 + D_\alpha^i(x, y)z_j^3] + \sum_{k=1}^{n_i} {}_k \tilde{C}_\alpha^i(x, y) \right\}_{i+c} \\ u_z(x, y, z) &= [ w^0(x, y) ]_0 + \left\{ [b^i(x, y)z + \sum_{k=1}^{n_i} {}_k \tilde{b}^i(x, y)z] + [c^i(x, y)z^2 + \sum_{k=1}^{n_i} {}_k \tilde{c}^i(x, y)z^2] + [d^i(x, y)z^3 + e^i(x, y)z^4 + \sum_{k=1}^{n_i} {}_k \tilde{d}^i(x, y)] \right\}_{i+c} \end{aligned} \quad (12)$$

Contributions  $[...]_0$  are the same as ZZA, while  ${}_k \tilde{B}_\alpha^i$ ,  $C_\alpha^i$ ,  ${}_k \tilde{C}_\alpha^i$  assume the same purpose as  $\Phi_\alpha^k$ ,  $C_\alpha^i$  and  ${}_k C_u^k$  inside ZZA,  ${}_k \tilde{b}^i$  and  ${}_k \tilde{c}^i$  perform the same function as  $\Omega^k$  and  $\Psi^k$  while  ${}_k \tilde{d}^i$  the function of  $C_\zeta^k$  because once redefined at material interfaces they allow to satisfy the continuity of interlaminar stresses and of displacements. Again  $C_\alpha^i$ ,  $D_\alpha^i$ ,  $b^i$ ,  $c^i$ ,  $d^i$  and  $e^i$  allow stress boundary conditions (7) and local equilibrium equations (8) to be met. Therefore similar to ZZA the redefinition of coefficients allows the representation to vary according to the conditions imposed. In details,  $b^i$  and  $c^i$  enable the fulfillment of stress boundary conditions relating to  $\sigma_{\zeta\zeta}$  and  $\sigma_{\zeta\zeta,\zeta}$  at the lower bounding face, then they are assumed to vanish in subsequent layers. Coefficients  $C_\alpha^i$ ,  $D_\alpha^i$ ,  $d^i$  and  $e^i$  allow to satisfy (8) at two points per layer, excluding the upper layer, and also enable stress-free boundary conditions on  $\sigma_{\alpha\zeta}$  and three equilibrium equations to be satisfied at a single point for the bottom layer. The remaining variables allow to meet three equilibrium equations at a single point across the upper layer and the stress boundary conditions on the upper surface. The present ZZA\* theory and other subsequent theories that also do not explicitly encompass zigzag functions can be still considered as physically-based zig-zag theories, because constraints are enforced in order to determine the expressions of coefficients.

In order to improve accuracy, the intermediate layers and the last one can be subdivided each into two or more computational layers, so that more equilibrium points can be enforced and, consequently, the representation order can be increased (but not necessarily, because coefficients can be evaluated at different positions using the same power of the thickness coordinate). To enable decomposition into computational layers, a sufficient number of contributions must be contained in the displacements field so an appropriate expansion order of summations in (12) has to be chosen. However, it will be shown by the present numerical results that even for the challenging benchmarks considered, just a third/fourth order overall representation is required to obtain very accurate results.

The new theories developed forward in section 3 of this paper will be aimed to prove that there is no need to assign a specific role to each coefficient, as just done for ZZA\_RDF (explained in section 2.3), that the order and type of representation can arbitrarily vary and independently for the single displacement and in a more general way that zig-zag layerwise contributions don't have to be incorporated explicitly (like for ZZA\*).

Numerical illustrations will show that ZZA\* and the new theories with the features just mentioned achieve the same accuracy of ZZA with a lower processing time, but their most important advantage is that the computational effort of the preparation phase, which is performed once and for all via symbolic calculus, decreases strongly.

## 2.5 HWZZ mixed theory

This theory was developed in [25] as a mixed Hu-Washizu version of ZZA wherein displacement strain and stress fields are assumed separately from each other in order to limit the computational cost while maintaining accuracy. For this purpose, only the contributions of each field deemed essential are preserved. Displacements derive from those of ZZA neglecting zig-zag contributions by  $\Omega^k$ , along with higher-order and adaptive contributions  $Oz^4 \dots$  and  $Oz^5 \dots$  (10) because numerical test have shown their secondary importance for displacements, while they remain of primary importance for stress fields. Consistent with these assumptions, no decomposition into computational layers is allowed for displacements, so also contributions  $C_u^k$ ,  $C_v^k$ ,  $C_w^k$  are omitted, then the displacement field simplifies to

$$u_\alpha(x, y, z) = [ u^0(x, y) + z(\Gamma_\alpha^0(x, y) - w^0(x, y)_{,\alpha}) ]_0 + [ C_\alpha^i(x, y)z^2 + D_\alpha^i(x, y)z^3 ]_i + [ \sum_{k=1}^{n_s} \Phi_\alpha^k(x, y)(z - z_k)H_k(z) ]_k \quad (13)$$

$$u_\zeta(x, y, z) = [ w^0(x, y) ]_0 + [ b^i(x, y)z + c^i(x, y)z^2 + d^i(x, y)z^3 + e^i(x, y)z^4 ]_i + [ \sum_{k=1}^{n_s} \Psi^k(x, y)(z - z_k)H_k(z) ]_k$$

Out-of-plane strains  $\varepsilon_{zz}$ ,  $\gamma_{xz}$ ,  $\gamma_{yz}$ , are obtained from those of ZZA neglecting zig-zag contributions by  $\Omega^k$ , but preserving those by  $C_u^k$ ,  $C_v^k$ ,  $C_w^k$  that enable decomposition into computational layers, while in-plane strains  $\varepsilon_x$ ,  $\varepsilon_y$ ,  $\varepsilon_{xy}$  directly follow from (13) and from strain-displacement relations. Once defined strains in this way, membrane stresses  $\sigma_{xx}$ ,  $\sigma_{yy}$ ,  $\sigma_{xy}$  are derived in a straightforward way from stress-strain relations, while out-of-plane stresses  $\sigma_{xz}$ ,  $\sigma_{yz}$ ,  $\sigma_{zz}$  are obtained by integrating local equilibrium equations, in order to recovery small stress jumps resulting from omission of contributions by  $\Omega^k$  in (13).

## 2.6 Theories HWZZ\_RDF, ZZA\*\_43 and HSDT\_34

A mutation of HWZZ, named HWZZ\_RDF is assessed, whose master displacement, strain and stress fields are the same of HWZZ, except for terms  $c^i$  which are calculated for  $i > 1$  by imposing the continuity of the transverse normal stress gradient at the interfaces, instead of imposing the fulfillment of local equilibrium equations. HWZZ\_RDF is considered together with other variants discussed forward in order to prove that it is unnecessary to assign a specific role to every single coefficient, instead the role can be freely exchanged without any accuracy loss, i.e. regardless of which coefficient is defined by imposing any of (7) to (9) and (11).

The results of theories ZZA\*\_43 and HSDT\_34 developed by the authors in a paper that is nearing completion are presented in the numerical applications in order to verify together with the new theories developed in section 3 that order and form of representation of displacements across the thickness can be changed freely, provided that a sufficient number of coefficients is incorporated so as to allow the fulfillment of (7) to (9) and (11). The features of these theories are summarized forward, since they provide rather accurate results and therefore can be used in practical applications.

ZZA\*\_43 is a reconstruction of ZZA\* which is obtained assuming each in-plane displacements as a fourth-order piecewise polynomial across the thickness, while the transverse displacement is assumed as a piecewise cubic polynomial:

$$u_\alpha(x, y, z) = [ u^0(x, y) + z(\Gamma_\alpha^0(x, y) - w^0(x, y)_{,\alpha}) ]_0 + \{ \sum_{k=1}^{n_s} k \tilde{B}_\alpha^i(x, y)z + [C_\alpha^i(x, y)z^2 + D_\alpha^i(x, y)z^3 + E_\alpha^i(x, y)z^4] + \sum_{k=1}^{n_s} k \tilde{C}_\alpha^i(x, y) \}_{i+\zeta} \quad (14)$$

$$u_\zeta(x, y, z) = [ w^0(x, y) ]_0 + \{ [b^i(x, y)z + \sum_{k=1}^{n_s} k \tilde{b}^i(x, y)z] + [c^i(x, y)z^2 + \sum_{k=1}^{n_s} k \tilde{c}^i(x, y)z^2] + [d^i(x, y)z^3] + \sum_{k=1}^{n_s} k \tilde{d}^i(x, y) \}_{i+\zeta}$$

Namely, the expansion order of displacements is reversed with respect to ZZA\*, while in accordance with it zig-zag functions aren't explicitly incorporated since their role is played by coefficients to be redefined across the thickness. As in ZZA\*, terms  ${}_k\tilde{B}_\alpha^i$ ,  $C_\alpha^i$ ,  ${}_k\tilde{C}_\alpha^i$  play the role that in ZZA is played by  $\Phi_\alpha^k$ ,  $C_\alpha^i$  and  ${}_kC_u^k$ , while  ${}_k\tilde{b}^i$  and  ${}_k\tilde{c}^i$  play the same role as  $\Omega^k$ ,  $\Psi^k$  and  ${}_k\tilde{d}^i$  play the same role of  $C_\alpha^k$ . Terms  $C_\alpha^i$ ,  $D_\alpha^i$ ,  $E_\alpha^i$ ,  $b^i$ ,  $c^i$  and  $d^i$  allow to satisfy and therefore are defined by local stress boundary conditions (7) and local equilibrium equations (8). However, numerical tests have shown that even permuting the role of coefficients, the result does not change, so what has been said previously about the role of the single coefficients can be varied arbitrarily, therefore it is not even necessary to explicitly define the functions of each one. As an example, the results of a variant ZZA\*\_43PRM, which is obtained assuming  ${}_k\tilde{B}_\alpha^i$  to play as  $C_\alpha^i$  of ZZA,  ${}_k\tilde{C}_\alpha^i$  to play as  $\Phi_\alpha^k$ ,  $C_\alpha^i$  as  ${}_kC_u^k$ ,  ${}_k\tilde{b}^i$  as  $C_\alpha^k$  and  ${}_k\tilde{c}^i$ ,  ${}_k\tilde{d}^i$  to play as  $\Omega^k$ ,  $\Psi^k$ , respectively, are reported in the numerical applications, which appear undistinguishable from those of ZZA\*\_43.

HSDT\_34 is a simplified theory derived as a particularization of ZZA starting from cubic in-plane displacements and a fourth-order transverse displacement, which get a piecewise variation in absence of zig-zag functions by virtue of the redefinition of coefficients, which for this reason have a superscript i:

$$\begin{aligned} u_\alpha(x, y, z) &= [u^0(x, y) + z(\Gamma_\alpha^0(x, y) - w^0(x, y)_{,\alpha})]_0 + B_\alpha^i(x, y)z + C_\alpha^i(x, y)z^2 + D_\alpha^i(x, y)z^3 \\ u_\zeta(x, y, z) &= [w^0(x, y)]_0 + b^i(x, y)z + c^i(x, y)z^2 + d^i(x, y)z^3 + e^i(x, y)z^4 \end{aligned} \quad (15)$$

This theory is considered for the twofold purpose of assessing whether accurate results can get by reducing the order of representation with respect to previous theories and of demonstrating through numerical applications that redefinition of coefficients is the key aspect that enables to improve accuracy, as it transforms a poor theory that without redefining the coefficients is a ESL into a layerwise one, and which also allows the elimination of zig-zag functions and still respecting (9), so ultimately confirming the results of other theories of this paper.

## 2.7 HWZZM and HWZZM\* mixed theories

This theory was constructed in [25] starting from the same assumptions of HWZZ but using different zig-zag functions, in order to show that the choice of these functions is immaterial since the same results of ZZA and ZZA\* are achieved whenever constraints (7) to (9) and (11) are simultaneously enforced. HWZZM is characterized by the following displacement field

$$\begin{aligned} {}^3u_\alpha(x, y, z) &= [u^0(x, y) + z(\Gamma_\alpha^0(x, y) - w^0(x, y)_{,\alpha})]_0 + [F_\alpha^i(z)]_i + [A_k^{u_\alpha}(z)[\frac{2z}{z_{k+1} - z_k} - \frac{z_{k+1} + z_k}{z_{k+1} - z_k}] + C_\alpha^k(x, y)]_c \\ {}^3u_\zeta(x, y, z) &= [w^0(x, y)]_0 + [F^\zeta(z)]_i + [A_k^{u_\zeta}(z)[\frac{2z}{z_{k+1} - z_k} - \frac{z_{k+1} + z_k}{z_{k+1} - z_k}] + B_k^{u_\zeta}(z)[\frac{(2z)^2}{z_{k+1} - z_k}] + C_\zeta^k(x, y)]_c \end{aligned} \quad (16)$$

from which expressions out-of-plane strains  $\mathcal{E}_{zz}$ ,  $\mathcal{Y}_{xz}$ ,  $\mathcal{Y}_{yz}$  are derived and from which its simplified counterpart used for obtaining membrane strains  $\mathcal{E}_x$ ,  $\mathcal{E}_y$ ,  $\mathcal{E}_{xy}$  follows in a straightforward way by neglecting adaptive contributions as in (13)

(here  ${}^3(\cdot)$  states that displacements refer to the computational layer  $\mathfrak{S}$ ). It could be noticed that layerwise functions in (16) derive from Murakami's zig-zag functions  $M^k(z) = (-1)^k \zeta^k$  assuming

$$\zeta^k = a^k z - b^k, a^k = \frac{2}{z_{k+1} - z_k}, b^k = \frac{z_{k+1} + z_k}{z_{k+1} - z_k} \quad (16')$$

HWZZM is still a physically-based zig-zag theory because expression of amplitudes  $A_k^{u_\zeta}$  and  $B_k^{u_\zeta}$  are not assumed a priori, but instead they are derived at each interface by enforcing the fulfilment of stress compatibility conditions (9), therefore all remains completely similar to ZZA.

As for HWZZ, membrane stresses  $\sigma_{xx}$ ,  $\sigma_{yy}$ ,  $\sigma_{xy}$  derive from stress-strain relations and the strains obtained as outlined above, while out-of-plane master stresses come from integration of local equilibrium equations.

In [25], various theories have been derived from HWZZM by assuming a priori and differently from each other the expressions of amplitudes  $A_k^{u_\alpha}$ ,  $A_k^{u_\zeta}$ ,  $B_k^{u_\zeta}$  that characterize the displacement components (16). Because these theories have proven to be much less accurate than theories where zig-zag amplitudes are defined on a physical basis, they are not considered in this paper.

Another mixed theory, called HWZZM\*, which is retaken from [25], is considered for sake of comparison. It is obtained starting from the following displacement field which, similarly to that of ZZA\*, does not explicitly contain any zig-zag function:

$$u_\alpha(x, y, z) = [ u^0(x, y) + z(\Gamma_\alpha^0(x, y) - w^0(x, y)_{,\alpha}) ]_0 + \left\{ \sum_{k=1}^{n_\alpha} {}_k\tilde{B}_\alpha^i(x, y)z \right\}_c + \left\{ [C_\alpha^i(x, y)z^2] + [D_\alpha^i(x, y)z^3] \right\}_i \tag{16''}$$

$$u_\zeta(x, y, z) = [ w^0(x, y) ]_0 + \left\{ [b^i(x, y)z] + [c^i(x, y)z^2] + [d^i(x, y)z^3] + e^i(x, y)z^4 \right\}_i + \left\{ \sum_{k=1}^{n_\alpha} {}_k\tilde{b}^i(x, y)z \right\}_c$$

Similarly to HWZZ and HWZZM, no decomposition into mathematical layers is allowed for the displacement field of HWZZM\* and  ${}_k\tilde{C}_\alpha^i$ ,  ${}_k\tilde{C}_\alpha^i$ ,  ${}_k\tilde{d}^i$  are omitted. In-plane master strains are still obtained by (16') while  ${}_k\tilde{C}_\alpha^i$  and  ${}_k\tilde{d}^i$  are restored for master out-of-plane ones, since subdivision into computational layers is allowed for these strains. Again, in-plane stresses are obtained from stress-strain relations, while  $\sigma_{xz}$ ,  $\sigma_{yz}$ ,  $\sigma_{zz}$  are computed by integration of (8). Numerical discussion will show that also HWZZM\* obtains results indistinguishable from those of ZZA and other higher-order theories, so corroborating that zig-zag functions can be omitted without any loss of accuracy if the full set of physical constrains (7-9, 11) is enforced and coefficients are redefined layer-by-layer.

### III. NEW THEORIES OF THIS PAPER

Theories are now introduced which are aimed at contributing to demonstrate that the representation form of the displacement field can be assumed arbitrarily whenever the full set of constraints (7) to (9) and (11) is enforced and the coefficients of the representation are redefined across the thickness. Under these conditions, it is aimed to show that the explicit incorporation of zig-zag contributions is unnecessary.

Firstly, two quite general theories retaken from a previous paper recently submitted and called ZZA-XX and ZZA-XX' are here reported which are considered in the numerical applications. The displacement field of ZZA-XX is defined as an infinite series of products of initially unknown amplitudes and exponential functions of the thickness coordinate  $z_i$ :

$$u_\alpha(x, y, z) = \left[ \sum_{k=1}^{\infty} C_{k-\alpha}^i(x, y)e^{(k z_i/h_i)} \right]_{\mathfrak{Z}} + \sum_{j=1}^{\mathfrak{Z}} D_{j-\alpha}^i(x, y) \tag{17}$$

$$u_\zeta(x, y, z) = \left[ \sum_{k=1}^{\infty} C_{k-\zeta}^i(x, y)e^{(k z_i/h_i)} \right]_{\mathfrak{Z}} + \sum_{j=1}^{\mathfrak{Z}} D_{j-\zeta}^i(x, y)$$

Coefficients are redefines for each computational layer  $\mathfrak{Z}$  of thickness  $h_i$  and calculated by imposing the full set of physical constrains (7-9, 11), where the expansion order can be chosen arbitrary by user, even if at least (7-9, 11) have to be imposed to obtain maximal accuracy. The displacement field of ZZA-XX' is:

$$u_\alpha(x, y, z) = \left[ \sum_{k=1}^{\infty} C_{k-\alpha}^i(x, y)z^{(k)} \right]_{\mathfrak{Z}} + \sum_{j=1}^{\mathfrak{Z}} D_{j-\alpha}^i(x, y) \tag{17'}$$

$$u_\zeta(x, y, z) = \left[ \sum_{k=1}^{\infty} C_{k-\zeta}^i(x, y)z^{(k)} \right]_{\mathfrak{Z}} + \sum_{j=1}^{\mathfrak{Z}} D_{j-\zeta}^i(x, y)$$

and the meaning of symbols if the same of (17). Starting from ZZA-XX and ZZA-XX' more general theories can be obtained, whose displacement field is assumed differently from one another and differently for even and odd layers. Such theories can be viewed as particularizations of the general representation

$$u_\alpha(x, y, z) = [ u_\alpha^0(x, y) + z(\Gamma_\alpha^0(x, y) - w^0(x, y)_{,\alpha}) ]_0 + [ \sum_{k=1}^{\mathfrak{Z}} C_{k-\alpha}^i(x, y)^i F_\alpha^k(z) + C_\alpha^i ]_{i;c} \tag{17''}$$

$$u_\zeta(x, y, z) = [ w^0(x, y) ]_0 + [ \sum_{k=1}^{\mathfrak{Z}} D_{k-\zeta}^i(x, y)^i G_\zeta^k(z) + C_\zeta^i ]_{i;c}$$

obtained through a different specification of  ${}^iF_k^\alpha$  and  ${}^iG_k$ , respectively for the in-plane and the transverse displacement component. Four different particularizations ZZA-X1 to ZZA-X4 have been so far already considered by the authors, to which another 4 new ones will be added here. Those already considered previously are particularized from (17) as follows:

ZZA\_X1

$$\begin{aligned} & \text{odd layers} & u_\alpha \triangleright {}^iF_\alpha^k &= \{z^k \quad (k=1,2,3)\} \\ & \text{even layers} & u_\beta \triangleright {}^iF_\beta^k &= \{z^k \quad (k=1,2,3)\} \\ & (i=2,4,\dots) & u_\zeta \triangleright {}^iG^k &= \left\{ \begin{matrix} z^{(k+1)/2} \text{ if } k=1,3 \\ e^{(kz/(2h))} \text{ if } k=2 \end{matrix} \right. (k_{\max}=3) \end{aligned} \quad (18)$$

ZZA\_X2

$$\begin{aligned} & \text{odd layers} & u_\alpha \triangleright {}^iF_\alpha^k &= \{z^k \quad (k=1,2,3)\} \\ & \text{even layers} & u_\beta \triangleright {}^iF_\beta^k &= \left\{ \begin{matrix} z^{(k+1)/2} \text{ if } k=1,3 \\ e^{(kz/(2h))} \text{ if } k=2 \end{matrix} \right. (k_{\max}=3) \\ & (i=2,4,\dots) & u_\zeta \triangleright {}^iG^k &= \left\{ \begin{matrix} z^{(k+1)/2} \text{ if } k=1,3 \\ e^{(kz/(2h))} \text{ if } k=2,4 \end{matrix} \right. (k_{\max}=4) \end{aligned} \quad (19)$$

ZZA\_X3

$$\begin{aligned} & \text{all layers} & u_\alpha \triangleright {}^iF_\alpha^k &= \left\{ \begin{matrix} z^{(k+1)/2} \text{ if } k=1,3 \\ e^{(kz/(2h))} \text{ if } k=2 \end{matrix} \right. (k_{\max}=3) \\ & (i=1,2,3,4,\dots) & u_\beta \triangleright {}^iF_\beta^k &= \left\{ \begin{matrix} z^{(k+1)/2} \text{ if } k=1,3 \\ e^{(kz/(2h))} \text{ if } k=2 \end{matrix} \right. (k_{\max}=3) \\ & & u_\zeta \triangleright {}^iG^k &= \left\{ \begin{matrix} z^{(k+1)/2} \text{ if } k=1,3 \\ e^{(kz/(2h))} \text{ if } k=2,4 \end{matrix} \right. (k_{\max}=4) \end{aligned} \quad (20)$$

ZZA\_X4

$$\begin{aligned} & \text{odd layers} & u_\alpha \triangleright {}^iF_\alpha^k &= \{z^k \quad (k=1,2,3)\} \\ & \text{even layers} & u_\beta \triangleright {}^iF_\beta^k &= \left\{ \begin{matrix} z/h \sin(z/h) \text{ if } k=2 \\ e^{(kz/(2h))} \text{ if } k=3 \end{matrix} \right. (k_{\max}=3) \\ & (i=2,4,\dots) & u_\zeta \triangleright {}^iG^k &= \left\{ \begin{matrix} z^k \text{ if } k=1,3 \\ e^{(kz/(2h))} \text{ if } k=2,4 \end{matrix} \right. (k_{\max}=4) \end{aligned} \quad (21)$$

Hereafter, four new theories ZZA\_X1\* to ZZA\_X4\* are considered. They are new variants of (17'') that don't contain any zig-zag functions. Like (18) to (21), their purpose is to demonstrate what claimed from theoretical standpoint, i.e. that through-the-thickness representations can be chosen arbitrary for each displacements and from point to point, without any loss of accuracy. It will be shown that such theories will provide results indistinguishable from others obtained by other higher-order theories, if coefficients are redefined layer-by-layer across the thickness and are calculated by imposing the fulfillment of (7) to (9) and (11):

ZZA\_X1\*

$$\begin{aligned} & \text{odd layers} & u_\alpha \triangleright {}^iF_\alpha^k &= \{z^k \quad (k=1,2,3)\} \\ & \text{even layers} & u_\beta \triangleright {}^iF_\beta^k &= \left\{ \begin{matrix} z^{(k+1)/2} \text{ if } k=1,3 \\ e^{(kz/(2h))} \text{ if } k=2 \end{matrix} \right. (k_{\max}=3) \\ & (i=2,4,\dots) & u_\zeta \triangleright {}^iG^k &= \{z^k \quad (k=1,2,3,4)\} \end{aligned} \quad (22)$$

ZZA\_X2\*

$$\begin{aligned} & \text{odd layers} & u_\alpha \triangleright {}^iF_\alpha^k &= \{z^k \quad (k=1,2,3)\} \\ & \text{even layers} & u_\beta \triangleright {}^iF_\beta^k &= \left\{ \begin{matrix} z^{(k+1)/2} \text{ if } k=1,3 \\ e^{(kz/(2h))} \text{ if } k=2 \end{matrix} \right. (k_{\max}=3) \\ & (i=2,4,\dots) & u_\zeta \triangleright {}^iG^k &= \left\{ \begin{matrix} z^{(k+1)/2} \text{ if } k=1,3 \\ e^{(kz/(2h))} \text{ if } k=2,4 \end{matrix} \right. (k_{\max}=4) \end{aligned} \quad (23)$$

$$\begin{aligned}
 & \text{ZZA\_X3*} \\
 \text{all layers} & \quad u_\alpha \triangleright {}^i F_\alpha^k = \begin{cases} z^{(k+1)/2} & \text{if } k=1,3 \\ e^{(kz/(2h))} & \text{if } k=2 \end{cases} (k_{\max}=3) \\
 & \quad u_\beta \triangleright {}^i F_\beta^k = \begin{cases} z/h & \text{if } k=2 \\ \sin(z/h) & \text{if } k=3 \end{cases} (k_{\max}=3) \\
 (\text{i}=1,2,3,4,\dots) & \quad u_\zeta \triangleright {}^i G^k = \begin{cases} z^{(k+1)/2} & \text{if } k=1,3 \\ e^{(kz/(2h))} & \text{if } k=2,4 \end{cases} (k_{\max}=4) \\
 & \text{ZZA\_X4*} \\
 \text{even layers} & \quad u_\alpha \triangleright {}^i F_\alpha^k = \begin{cases} z^k & \text{if } k=1,3 \\ e^{(z/h)} & \text{if } k=2 \end{cases} (k_{\max}=3) \quad \text{odd layers} \quad u_\alpha \triangleright {}^i F_\alpha^k = \{z^k \quad (k=1,2,3)\} \\
 (\text{i}=2,4,\dots) & \quad u_\beta \triangleright {}^i F_\beta^k = \begin{cases} z/h & \text{if } k=2 \\ \sin(z/h) & \text{if } k=3 \end{cases} (k_{\max}=3) \quad (\text{i}=1,3,\dots) \quad u_\beta \triangleright {}^i F_\beta^k = \begin{cases} z/h & \text{if } k=2 \\ \sin(z/h) & \text{if } k=3 \end{cases} (k_{\max}=3) \\
 & \quad u_\zeta \triangleright {}^i G^k = \{z^k \quad (k=1,2,3,4)\} \quad u_\zeta \triangleright {}^i G^k = \begin{cases} z^k & \text{if } k=1,3 \\ e^{(z/h)} & \text{if } k=2,4 \end{cases} (k_{\max}=4)
 \end{aligned} \tag{24}$$

#### IV. NUMERICAL ASSESSMENTS AND DISCUSSION

Henceforth the accuracy of theories will be assessed considering a number of elasto-static challenging benchmarks having pronounced layerwise effects deriving from geometric and material properties, lay-ups and loading that are often typical of cases of industrial interest. These benchmarks are selected as they require simultaneously a very accurate modeling of transverse normal deformation effects. Of interests, here are transverse anisotropy effects, accordingly strong different elastic properties of layers are considered rather than ones from just reoriented layers, which is simply omitted. Cases are retaken from [24] and [25], wherein it is indicated who studied them previously.

The prefixed purpose of numerical illustrations is to show that refined physically-based zig-zag theories of this paper very accurately describe layerwise effects, with a smaller number of d.o.f. than widespread theories described in [5-8], [11-17], whenever the full set of physical constraints (7) to (9) and (11) is enforced, which lets the present theories to assume the appellation of physically-based, the following holds.

(i) The functions expressing the variation of displacements across the thickness can be arbitrarily chosen without having any difference in the results; (ii) also zig-zag functions can be arbitrarily chosen and (iii) even be omitted, if a sufficient number of coefficients is still considered, whose expressions are re-determined across the thickness, with the advantage of containing computational of phases carried out in symbolic form; (iv) a different representation varying from region to region across the thickness can be freely chosen as desired and different zig-zag functions can be assumed for each single displacement (variable-kinematics form) without any accuracy loss, (v) a specific role need not be assigned to individual coefficients whenever their expressions are re-defined across the thickness by imposing (7) to (9) and (11), as the role can be freely exchanged if overall the same conditions are imposed.

Because industrial designers are interested to know whether lower order theories of low cost can be used to carry out analysis, the present study consider these theories in order to confirm that, as shown in literature, they can be accurate for certain cases but not in general; consequently, (vi) a partial fulfilment of (7) to (9) and (11) even with a fairly high degree of representation implies a loss of validity of (i) to (v), so that accuracy back to being strongly dependent upon the representation adopted.

#### 4.1 CASE A

It concerns a simply supported sandwich beam under two half-waves sinusoidal loading applied at the upper face, with graphite-epoxy faces and foam core and a side length-to-thickness ratio of 10. This case is a modified version of that formerly studied in [25], in order to prove that because of the presence of an inflection point in the loading distribution the effects played by the transverse normal deformability on equilibrium of transverse shear and normal stresses are still equally enhanced. This is confirmed by the numerical results of Fig. 1 and Table 4a for this case because, indeed, inaccurate results are obtained by lower-order theories like MHWZZA, MHWZZA4, HRZZ, HRZZ4 but in particular, by MHR and MHR4 in mixed form that assume a polynomial or piecewise representation of the transverse displacement across the thickness, respectively and kinematic-based zig-zag functions. The reason is that such lower-order theories cannot accurately reproduce the trend of transverse normal and shear stresses across the thickness, not even when out-of-plane stresses are derived from the membrane components through the integration of local equilibrium equations. Errors cannot be recovered even when strain and stress fields are assumed apart and with an already rather high order, like in the case of mixed theory MHWZZA

that incorporates strains and stress fields of HWZZ, as well as also even when the transverse displacement comes from ZZA, as in the case of MHWZZA4, a sign that a description capable of representing the effects of normal transverse deformation and the relative stress is required without any simplification being used. The results of the theories considered in this paper reported in Fig. 1 and Table 4a leave out theories that had already demonstrated their inadequacy in [24,25]. These omitted theories are all those having simplifying assumptions that result in a poor description of displacement and stress fields, such as all kinematic based theories with immutable zigzag contributions because defined once and for all. Since errors characterize mixed theories HRZZ and HRZZ4 are lower than MHR and MHR4 that include Murakami’s zig-zag functions, it is demonstrated the superiority of physically-based theories over kinematic based ones. Results show that only higher-order adaptive theories (ZZA, ZZA\*, HWZZM, HWZZM\*, HWZZ, HSDT\_34, ZZA\*\_43, ZZA-XX, ZZA-XX’, ZZA\_RDF, HWZZ\_RDF, ZZA\_X1 to \_X4, ZZA\*\_43PRM and ZZA\_X1\* to X4\*), whose coefficients are redefined layer-by-layer across the thickness and that impose the fulfillment of full set of physical constraints (7) to (9) and (11) are always accurate and that their results are indistinguishable from one another. This therefore shows that zig-zag functions can be freely changed, so, even they can be assumed in Murakami’s form, provided that amplitudes are recalculated at each interface. Moreover, it is shown that they can be omitted if coefficients are recomputed across the thickness, as shown by the results of ZZA-X1 to ZZA-X4 and ZZA-X1\* to ZZA-X4\* having a different representation form for each displacement, which is differently assumed form point to point across the thickness.

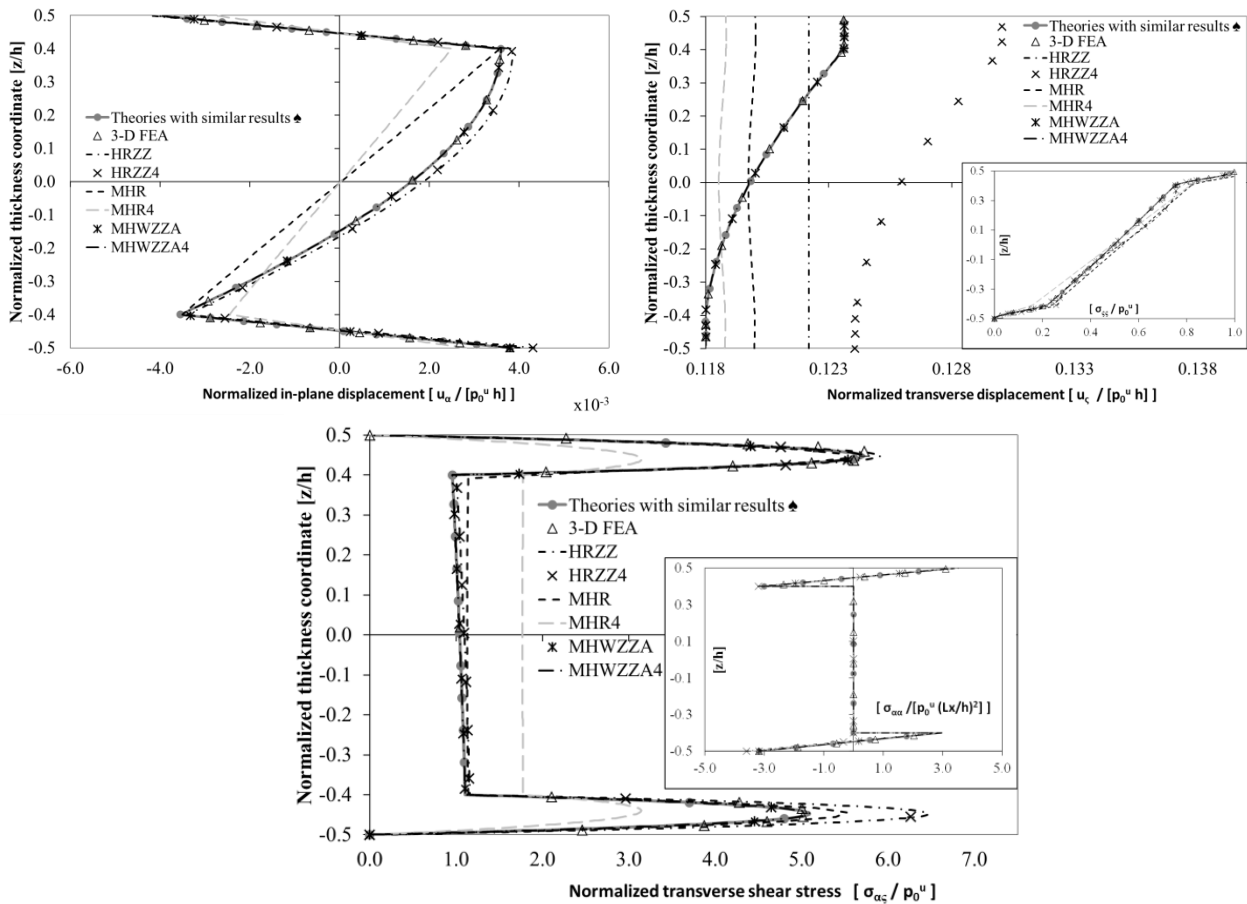


**FIGURE 1: Normalized in-plane displacement, transverse displacement, transverse shear stress, in-plane stress (in the inset) and transverse normal stress (in the inset) for case a. Symbol ♠ indicates that theories ZZA, ZZA\*, HWZZM, HWZZM\*, HWZZ, HSDT\_34, ZZA\*\_43, ZZA-XX, ZZA-XX’, ZZA\_RDF, HWZZ\_RDF, ZZA\_X1 to \_X4, ZZA\*\_43PRM and ZZA\_X1\* to X4\* obtain results which differ for less than 1%.**

Table 3, shows that processing time of higher-order theories is still always comparable to those of ESL and that lower-order ones, which however cannot obtain a similar or acceptable degree of accuracy, so their advantage in terms of computational burden is only apparent. It could be seen from Table 3 that anyway theories wherein zig-zag functions are omitted are the most efficient theories considered in this paper being able to achieve the same accuracy of theories incorporating zig-zag functions with a lower processing time.

**TABLE 3**  
**Processing time [s]; errors:  $\nabla > 3\%$ ;  $\ast > 10\%$ .**

Type	Theory	Features	Cases	a	b	c	d	e
New theories	FSDT	Reference theory		2.3014	2.3045	2.4710	5.9211	6.1245
	ZZA_X1*	Arbitrary representation		3.7673	3.7015	4.2532	11.4310	12.0417
	ZZA_X2*			3.8680	3.8254	4.3774	11.7316	12.3256
	ZZA_X3*			3.9032	3.8444	4.3979	11.9151	12.5217
	ZZA_X4*			3.8969	3.8535	4.4288	11.8392	12.4289
Mixed HR	HRZZ	Uniform $w^0$		$\nabla 5.3990\ast$	$\nabla 5.5423\ast$	$\nabla 7.4582\ast$	$\nabla 18.4274\ast$	$\nabla 18.2287\ast$
	HRZZ4	Polynomial $w^4$		$\nabla 5.4094\ast$	$\nabla 5.2737\ast$	$\nabla 11.0258\ast$	$\nabla 18.9174\ast$	$\nabla 18.4489\ast$
	MHR	Murakami's zig zag $u^3, v^3$		4.3663	$\nabla 4.5619\ast$	$\nabla 4.8186\ast$	$\nabla 6.7118\ast$	$\nabla 6.9651\ast$
	MHR4	Murakami's zig zag $u^3, v^3, w^4$		$\nabla 4.3310\ast$	$\nabla 4.3291\ast$	$\nabla 4.9692\ast$	$\nabla 6.1582\ast$	$\nabla 6.4367\ast$
Mixed HW	HWZZ			4.4949	4.5726	5.2894	12.0471	12.3960
	HWZZ_RDF			4.3621	4.2988	4.9147	13.2034	13.9751
	HWZZM*	No zig-zag functions		3.6891	3.6223	4.1572	11.1507	11.7533
	HWZZM	Murakami's zig zag $u^3, v^3, w^4$		4.0107	3.9760	4.5548	12.1959	12.8123
	MHWZZA			4.4726	$\nabla 4.6131\ast$	$\nabla 5.1828\ast$	$\nabla 7.2626\ast$	$\nabla 7.9157\ast$
	MHWZZA4			4.6211	$\nabla 4.7301\ast$	$\nabla 5.2798\ast$	$\nabla 7.1210\ast$	$\nabla 7.8126\ast$
	ZZA	Adaptive $u^3, v^3, w^4$		4.9770	4.9120	5.6127	15.0929	15.8988
	ZZA_RDF			4.7548	4.6900	5.3309	14.4480	15.1919
	ZZA*	No zig-zag functions $u^3, v^3, w^4$		3.7181	3.6988	4.2332	11.3110	11.9627
	HSDT_34			3.7371	3.6694	4.2077	11.3441	11.9652
	ZZA*_43	No zig-zag functions $u^4, v^4, w^3$		3.7393	3.7005	4.2142	11.3391	11.8843
	ZZA*_43PRM			3.7438	3.6955	4.2329	11.3713	11.9072
	ZZA_X1	Arbitrary representation		3.7705	3.7064	4.2545	11.4102	12.0588
	ZZA_X2			3.8508	3.7999	4.3686	11.6656	12.3498
	ZZA_X3			3.9127	3.8502	4.3945	11.9047	12.4688
	ZZA_X4			3.9074	3.8509	4.4108	11.9031	12.4591
	ZZA-XX	General representation		9.4659	9.3495	10.6582	28.5583	30.1960
	ZZA-XX'			9.2262	9.1041	10.3746	28.0411	29.4950

On a computer with quad-core CPU@2.60GHz, 64-bit OS and 8.00 GB RAM; FSDT shear correction factor 5/6.

**TABLE 4a**  
**Results for case a.**

Case a	Position	3-D FEA	Theories with similar results $\clubsuit$	HRZZ	HRZZ4	MHR	MHR4	MHWZZA	MHWZZA4
$u_a \times 10^{-3}$	up/min	-4.1022	-4.1021	-4.2829	-4.2703	-3.9624	-2.7736	-4.1093	-4.1112
	down/max	3.7999	3.7925	4.3434	4.3061	4.0179	2.8125	3.8025	3.8063
$u_\zeta \times 10^{-1}$	up	1.2362	1.2359	1.2220	1.3003	1.2002	1.1882	1.2358	1.2360
	down	1.1799	1.1796	1.2220	1.2406	1.1998	1.1878	1.1795	1.1797
	max	1.2364	1.2361	1.2220	1.3005	1.2004	1.1884	1.2360	1.2362
	min	1.1799	1.1796	1.2220	1.2406	1.1998	1.1878	1.1795	1.1797
$\sigma_{aa}$	up/max	3.4318	3.4329	3.5828	3.5722	3.3149	3.2517	3.4331	3.4328
	down/min	-3.1755	-3.1797	-3.6297	-3.5985	-3.3577	-3.4353	-3.1808	-3.1770
$\sigma_{a\zeta}$	max	5.7202	5.8346	6.4703	6.3773	5.5537	3.1530	5.7264	5.7349
$\sigma_{\zeta\zeta}$	up/max	1.0000	1.0000	1.0000	1.0000	1.0000	1.0000	1.0000	1.0000

Symbol  $\clubsuit$  indicates that theories ZZA, ZZA\*, HWZZM, HWZZM\*, HWZZ, HSDT\_34, ZZA\*\_43, ZZA-XX, ZZA-XX', ZZA\_RDF, HWZZ\_RDF, ZZA\_X1 to \_X4, ZZA\*\_43PRM and ZZA\_X1\* to X4\*obtain results which differ for less than 1%

4.2 CASE B

In this case the same sandwich beam of case a is considered, except that the lower face is assumed to be damaged, its mechanical properties being reduced of two order of magnitude, according to the ply-discount theory ( $E_{1111}$   $E_{1122}$   $E_{2222}$   $E_{1212}$  reduced by  $2 \cdot 10^{-2}$ ) because it happens often in practice, e.g. due to the impact of a foreign object that even if occurring only locally, it still represents an area where the analysis must be as accurate as possible, but also because the strong asymmetry of material properties enhances 3-D elastic effects, becoming a very severe test from the standpoint of theories.

The results for this case given in Fig. 2 and in Table 4b confirm the primary role played by a very accurate modelling of the transverse displacement once a marked difference of elastic properties of faces is considered. It can be seen that the through-thickness variation of the in-plane displacement is quite accurately predicted by all theories, so it does not represent a discriminating quantity, so different representations prove to be adequate. The opposite occurs instead for the transverse displacement, but for this case error on  $u_\zeta$  are not seen to reflect on out-of-plane stresses. Indeed, such stresses are quite accurately predicted also by MHR, MHR4, MHWZZA, MHWZZA4, HRZZ and HRZZ4 since the reduced elastic properties of the lower face, which are somewhat more similar to those of the core rather to those of the upper one, prevent the spreading across the thickness, causing their concentration near to it.

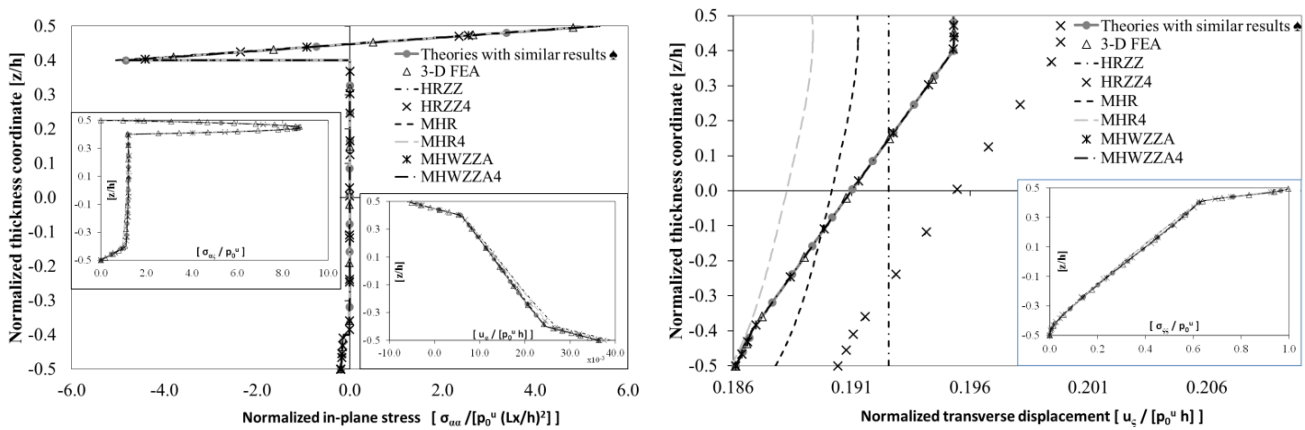


FIGURE 2: Normalized in-plane stress, in-plane displacement (in the inset), transverse shear stress (in the inset), transverse displacement and normalized transverse normal stress (in the inset) for case b.

TABLE 4b  
Results for case b.

Case b	Position	3-D FEA	Theories with similar results ♠	HRZZ	HRZZ4	MHR	MHR4	MHWZZA	MHWZZA4
$u_\alpha$ $\times 10^{-3}$	up/min	-7.3337	-7.3412	-6.4956	-6.4713	-6.2484	-6.5608	-6.3837	-6.3718
	down/max	37.6515	37.7012	38.8976	37.5123	36.1826	37.9917	36.3228	36.3345
$u_\zeta$ $\times 10^{-1}$	up	1.9529	1.9529	1.9257	1.9980	1.9124	1.8933	1.9529	1.9529
	down/min	1.8611	1.8609	1.9257	1.9041	1.8779	1.8591	1.8608	1.8609
	max	1.9533	1.9533	1.9257	1.9983	1.9128	1.8937	1.9533	1.9533
$\sigma_{\alpha\alpha}$	up/max	5.3383	5.3330	5.4319	5.4115	5.2253	5.2343	5.3446	5.3465
	down	-0.1926	-0.1925	-0.2062	-0.1989	-0.1918	-0.1919	-0.1966	-0.1921
	min	-4.8293	-4.8261	-5.0463	-4.9921	-4.8346	-4.8520	-4.8078	-4.8196
$\sigma_{\alpha\zeta}$	max	8.7600	8.8067	8.8180	8.7679	8.5258	8.8528	8.7773	8.7777
$\sigma_{\zeta\zeta}$	up	1.0000	1.0000	1.0000	1.0000	1.0000	1.0000	1.0000	1.0000
	max	1.0000	1.0000	1.0061	1.0107	1.0000	1.0000	1.0000	1.0000

Anyway, once again, the only theories shown capable of correctly reproducing stress and displacement through-thickness variations are shown to be ZZA, HWZZ together with all the remaining higher-order theories. The results also show that what claimed in (i) to (vi) holds also for this case since ZZA, ZZA\*, HWZZM, HWZZM\*, HWZZ, HSDT\_34, ZZA\*\_43, ZZA-XX, ZZA-XX', ZZA\_RDF, HWZZ\_RDF, ZZA\_X1 to \_X4, ZZA\*\_43PRM and ZZA\_X1\* to X4\* achieve the same accuracy degree, their results being indistinguishable from one another. Use of higher-order theories is still confirmed preferable to that of lower-order ones, both because the latter misestimate displacement and stress fields and do not provide advantages in terms of computational costs (see Table 3). As results from this table, higher-order theories that omit layerwise functions are the most efficient theories of this paper, having the same accuracy of other higher-order models and lower processing time.

### 4.3 CASE C

In this case, a similar simply supported sandwich structure with graphite-epoxy faces and foam core of previous cases a and b is still considered (dimension and material properties are reported in Table 2a). The structure is loaded by a step compressive loading on its upper and lower faces, as indicated in Table 2b. This type of load is considered because it shows stronger layerwise effects than those of sinusoidal loading considered in cases a and b.

Results of Fig. 3 and Table 4c for this case referring to  $u_\alpha$  and  $\sigma_{\alpha\zeta}$  are reported at  $x/L_x = 0$ , while those for  $u_\zeta$ ,  $\sigma_{\alpha\alpha}$  and  $\sigma_{\zeta\zeta}$  are reported at  $x/L_x = 0.25$ , because at these two positions they exhibit peaks. Despite the strong layerwise effects due to the loading considered, theories unexpectedly show results in a better agreement each other and with FEA 3-D than in the previous cases. Anyway, some errors are shown by lower-order theories, that is to say MHR, MHR4, MHWZZA, MHWZZA4, HRZZ, HRZZ4, as regards displacements across the core, as only ZZA, ZZA\*, HWZZM, HWZZM\*, HWZZ, HSDT\_34, ZZA\*\_43, ZZA-XX, ZZA-XX', ZZA\_RDF, HWZZ\_RDF, ZZA\_X1 to \_X4, ZZA\*\_43PRM and ZZA\_X1\* to X4\* turn out to be able to provide an adequate information in this case. From the standpoint of accuracy of theories, this is signing a strong case-dependence by loading, as it results from the comparison with previous cases a and b. Even if errors are not very large, theories based on Murakami's zig-zag function whose coefficients are not redefined across the thickness appear inadequate because in the present case the slope of in-plane and transverse displacements don't reverse at interfaces.

In the same way, theories which have a simplified kinematics of  $u_\zeta$  like MHR, MHR4, HRZZ, HRZZ4, MHWZZA and MHWZZA4 are inadequate, not even when using the best theories like ZZA, ZZA\*, HWZZM, HWZZM\*, HWZZ, HSDT\_34, ZZA\*\_43, ZZA-XX, ZZA-XX', ZZA\_RDF, HWZZ\_RDF, ZZA\_X1 to \_X4, ZZA\*\_43PRM and ZZA\_X1\* to X4\* as post-processors. Errors in  $u_\zeta$  reflect into an overestimation of the transverse shear stress across the upper face, which is more evident for theories MHWZZA and MHWZZA4, and in a underestimation by HRZZ and HRZZ4 across both faces. So this is signing that  $u_\zeta$  assumes a paramount importance under step loading. To highlight the largely case-sensitive behavior of theories based on simplifying hypotheses, and therefore the unpredictability of their predictions, it could be noted that while MHWZZA and MHWZZA4 inadequately predict the variation of the in-plane displacement across the core, their lower-order counterparts MHR, MHR4 give results much closer to FEA-3D due to a mutual compensation of errors.

Only higher-order adaptive theories (ZZA, ZZA\*, HWZZM, HWZZM\*, HWZZ, HSDT\_34, ZZA\*\_43, ZZA-XX, ZZA-XX', ZZA\_RDF, HWZZ\_RDF, ZZA\_X1 to \_X4, ZZA\*\_43PRM and ZZA\_X1\* to X4\*), whose coefficients are redefined layer-by-layer across the thickness and that impose the fulfillment of full set of physical constraints (7) to (9) and (11) appear always able to get accurate displacements and stresses. Indeed, their results are indistinguishable from one another and from those of 3-D FEA, irrespective of zig-zag functions or representation assumed. So ultimately this confirms that their choice is immaterial and so what claimed in (i) to (vi) also for this case.

The same still holds as regards the computational cost seen for the previous cases, because the little less expensive but inaccurate lower-order theories cannot provide real advantages over higher-order ones, see, Table 3. Higher-order theories that do not contain zig-zag functions are shown again to require a nearly or little more calculation time than their lower-order counterparts (which however are less accurate), proving to be the most efficient theories of this paper.

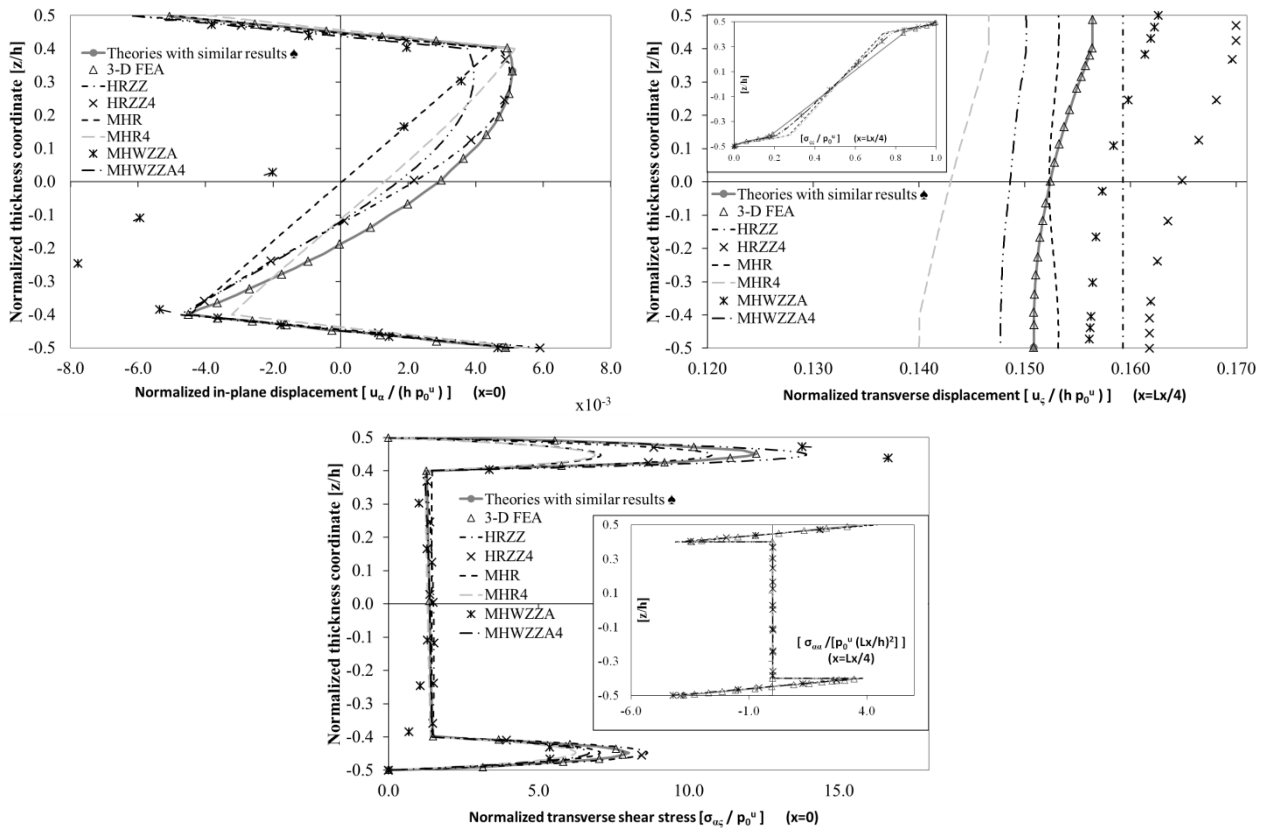


**FIGURE 3: Normalized in-plane displacement, transverse displacement, transverse shear stress, transverse normal and in-plane stresses (in the insets) for case c.**

**TABLE 4c  
Results for case c.**

Case c	Position	3-D FEA	Theories with similar results ♣	HRZZ	HRZZ4	MHR	MHR4	MHWZZA	MHWZZA4
$u_x$ $\times 10^{-3}$ ( $x=0$ )	up	-5.0694	-5.1284	-6.1288	-6.1299	-5.0448	-3.9548	-6.1457	-6.2844
	down	4.8842	4.8354	5.9176	5.9003	5.1157	5.5149	4.6516	4.9863
	max	5.0889	5.1345	5.9176	5.9003	5.1157	5.5149	4.6516	4.9863
	min	-5.0694	-5.1284	-6.1288	-6.1299	-5.0448	-3.9548	-7.7749	-6.2844
$u_z$ $\times 10^{-1}$ ( $x=Lx/4$ )	up	1.5639	1.5640	1.5928	1.6993	1.4660	1.5320	1.6264	1.5013
	down/min	1.5088	1.5089	1.5928	1.6178	1.4001	1.5316	1.5605	1.4769
	max	1.5641	1.5642	1.5928	1.6997	1.4661	1.5323	1.6264	1.5016
$\sigma_{aa}$ ( $x=Lx/4$ )	up/max	3.7846	3.7596	4.5093	4.5153	4.1485	4.0898	4.2213	4.2635
	down	-3.7772	-3.7316	-3.9002	-3.9081	-4.0382	-4.0905	-4.2200	-4.2622
	min	-3.7772	-3.7316	-4.1253	-4.1325	-4.0382	-4.0905	-4.2200	-4.2622
$\sigma_{a\zeta}$ ( $x=0$ )	max	12.2525	12.2550	10.7842	10.8634	7.0695	6.8761	17.4821	13.9216
$\sigma_{\zeta\zeta}$ ( $x=Lx/4$ )	up/max	1.0000	1.0000	1.0000	1.0000	1.0000	1.0000	1.0000	1.0000

**4.4 CASE D**

A propped-cantilever sandwich beam under uniform loading and with a length-to-thickness ratio  $l_x / h = 14.286$  is considered, whose geometric and material properties are indicated in Table 2a. Fig. 4 and Table 4d show the through-thickness variation of displacements and transverse shear and normal stresses for this case, formerly considered in [25], as predicted by the various theories considered in this paper. Although the structure is rather slim, major discrepancies still exist among the predictions of theories because strong layerwise effects still persist like in the thickest structures.

Because of this, simplified kinematics assumptions of theories MHR, MHR4, MHWZZA, MHWZZA4, HRZZ, HRZZ4 become completely inadequate, although in the literature it is often claimed that even ESL can be used when  $l_x / h$  similar to

the one is considered here. Moreover, the stress field is described in an imprecise way by all theories except by ZZA and theories ZZA\*, HWZZM, HWZZM\*, HWZZ, HSDT\_34, ZZA\*\_43, ZZA-XX, ZZA-XX', ZZA\_RDF, HWZZ\_RDF, ZZA\_X1 to \_X4, ZZA\*\_43PRM and ZZA\_X1\* to X4\*, which indeed provide indistinguishable results from each other. So, it is demonstrated what is claimed in this paper regarding the arbitrary choice of zig-zag functions and of the representation, provided that all physical constraints are contemporaneously satisfied. In particular, the transverse normal stress is misestimate by all lower-order theories. Nevertheless the slope of displacements reverses at both face-core interfaces, theories MHR and MHR4 based upon Murakami's zig-zag function incorrectly predict displacement and stress fields. Instead, theories whose coefficients are redefined layer-by-layer across the thickness by imposing the fulfilment of full set of physical constraints (7) to (9) and (11) are always accurate, irrespective of zig-zag functions or the representation assumed, so confirming what claimed in (i) to (vi). It is confirmed also for this case that higher-order theories are more efficient than lower-order ones, as shown by Table 3, and the most efficient are those that do not explicitly contain zig-zag functions, as they have the same accuracy but a lower processing time.

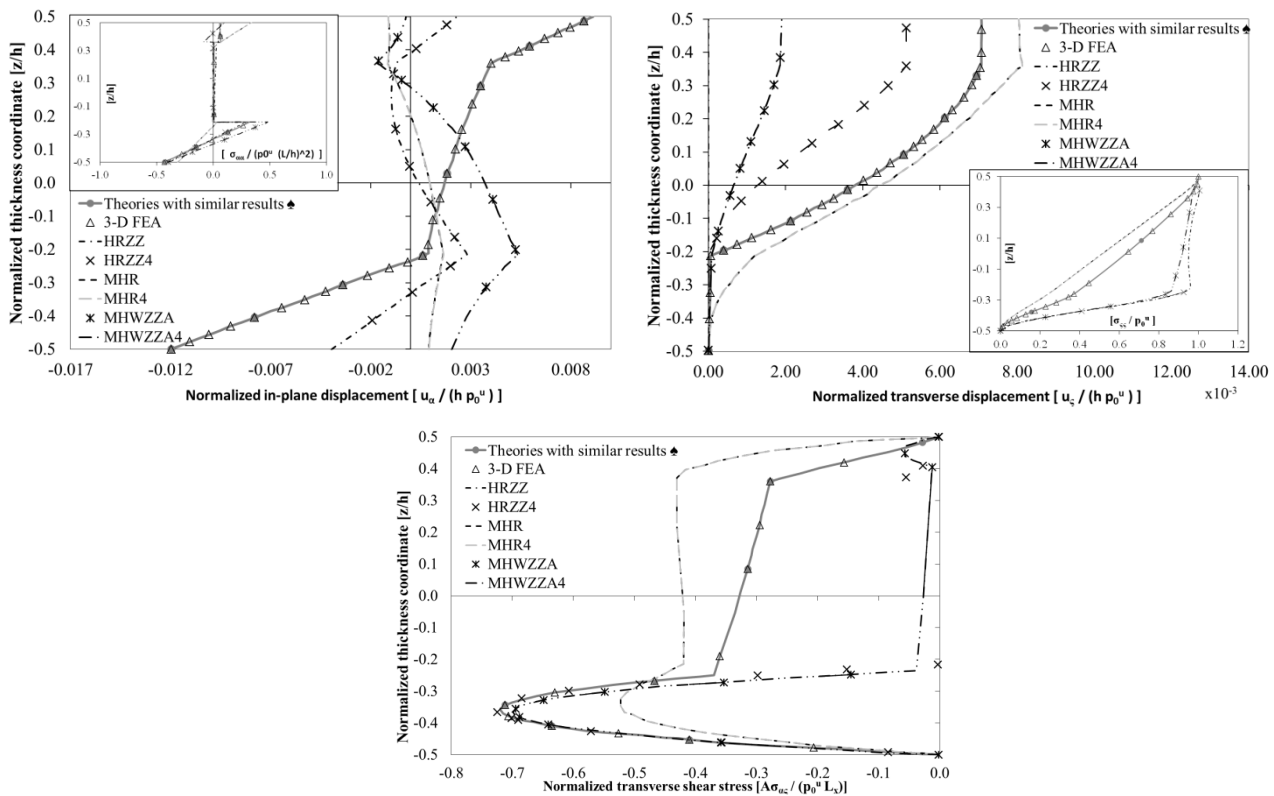


FIGURE 4: Normalized in-plane displacement, in-plane stress (in the inset), transverse displacement, transverse normal stress (in the inset), transverse shear stress for case d.

TABLE 4d  
Results for case d.

Case d	Position	3-D FEA	Theories with similar results ♣	HRZZ	HRZZ4	MHR	MHR4	MHWZZA	MHWZZA4
$u_x$ $\times 10^{-3}$	up	9.1138	9.1078	2.3007	2.2945	-1.1155	-1.1063	-0.2381	-0.2315
	down	-11.9627	-11.9506	-3.9677	-3.9760	0.9058	0.9143	2.0341	2.0360
	max	9.1138	9.1078	2.8215	2.8208	1.6311	1.6285	5.3391	5.3242
	min	-11.9627	-11.9506	-3.9677	-3.9760	-1.1393	-1.1367	-1.7104	-1.7185
$u_z$ $\times 10^{-3}$	up	7.0780	7.0543	0	5.0978	8.0429	8.0510	1.9002	1.9019
	max	7.0801	7.0815	0	5.1247	8.1313	8.1673	1.9002	1.9002
	down/min	0	0	0	0	0	0	0	0
$\sigma_{xx}$	up	0.0562	0.0554	0.0711	0.0717	0.3440	0.3453	0.1071	0.1061
	down/min	-0.4320	-0.4314	-0.3980	-0.3922	-0.3139	-0.3162	-0.4000	-0.4015
	max	0.3215	0.3252	0.2872	0.2839	0.3440	0.3453	0.4818	0.4808
$\sigma_{xz}$	min	-0.7192	-0.7189	-0.7200	-0.7245	-0.5228	-0.5168	-0.6989	-0.7043
$\sigma_{zz}$	up/max	1.0000	1.0000	1.0000	1.0000	1.0000	1.0000	1.0000	1.0000

4.5 CASE E

Now it is considered a propped-cantilever sandwich beam under uniform loading like for case d, but actually a thicker structure with  $l_x/h = 5.714$  and damaged lower face and core are considered, according to the ply-discount theory ( $E_{1111} E_{1122} E_{2222} E_{1212} 4 \cdot 10^{-2}$  for Layer 1,  $E_{1122} E_{2222} E_{1212} E_{1313} E_{2323} 2 \cdot 10^{-2}$  for Layer 2).

Given the strong discrepancies between the indications of the theories shown by the results of Fig. 5 and Table 4e, the present benchmark turns out to be decidedly challenging and therefore particularly selective and suited to highlight the discrepancies among lower- and higher-order theories. Again, only ZZA, ZZA\*, HWZZM, HWZZM\*, HWZZ, HSDT\_34, ZZA\*\_43, ZZA-XX, ZZA-XX', ZZA\_RDF, HWZZ\_RDF, ZZA\_X1 to \_X4, ZZA\*\_43PRM and ZZA\_X1\* to X4\* are capable to express the variation of displacement and stress fields everywhere by virtue of their better capacity to describe all the variations that occur in the displacement and stress fields, thanks to the possibility they offer of redefining the coefficients of representation in such a way as to satisfy all the requirements of the theory of elasticity.

MHR and MHR4 making use of Murakami's zig-zag functions appear decidedly inaccurate in this case, as they predict a wrong nearly uniform variation of in-plane displacements because of their too simple kinematics. Besides, all lower-order theories (MHR, MHR4, MHWZZA, MHWZZA4, HRZZ and HRZZ4) incorrectly predict the transverse shear stress and in a totally wrong way the transverse normal stress elsewhere across the thickness. Again, HRZZ (that assume a uniform  $u_z$  across the thickness) obtain the worst results as regards the transverse displacement. Table 3 shows again that the processing time of lower-order theories remains similar to that of higher-order adaptive theories, so, the former theories which are less accurate are not useful neither from the point of view of accuracy, nor from computational burden. It is also confirmed that higher-order physically-based zig-zag adaptive theories ZZA, ZZA\*, HWZZM, HWZZM\*, HWZZ, HSDT\_34, ZZA\*\_43, ZZA-XX, ZZA-XX', ZZA\_RDF, HWZZ\_RDF, ZZA\_X1 to \_X4, ZZA\*\_43PRM and ZZA\_X1\* to X4\* are the only always everywhere accurate and that their results are indistinguishable from each other. Higher-order theories without zig-zag functions are shown again as the most efficient theories of this paper.

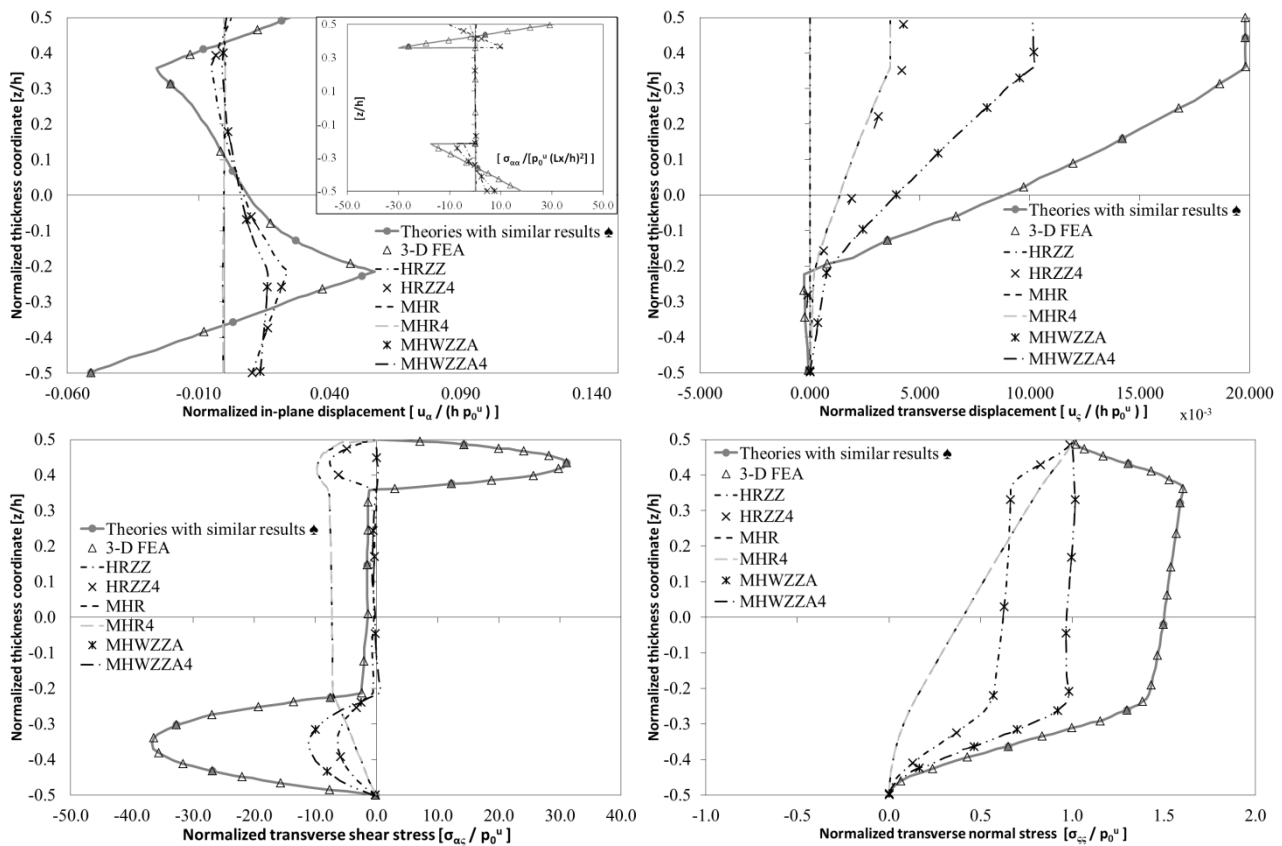


FIGURE 5: Normalized in-plane displacement and stress (in the inset), transverse displacement, transverse shear stress and transverse normal stress for case e.

**TABLE 4e**  
**Results for case e.**

Case e	Position	3-D FEA	Theories with similar results $\clubsuit$	HRZZ	HRZZ4	MHR	MHR4	MHWZZA	MHWZZA4
$u_\alpha$ $\times 10^{-2}$	up	2.4904	2.4922	0.2563	0.2542	-0.0264	-0.0262	0.0657	0.0656
	down	-5.1031	-5.1067	1.0438	1.0458	-0.0639	-0.0637	1.3600	1.3658
	max	5.7212	5.7306	2.3987	2.3922	0.0191	0.0191	1.6521	1.6626
	min	-5.1031	-5.1067	-0.5210	-0.5220	-0.0705	-0.0703	-0.1118	-0.1115
$u_\zeta$ $\times 10^{-2}$	up	19.8052	19.8180	0	4.2621	3.6543	3.6636	10.1240	10.1369
	down	0	0	0	0	0	0	0	0
	max	19.8219	19.8317	0	4.2701	3.6543	3.6636	10.2232	10.2440
	min	-0.2638	-0.2628	0	-0.1643	0	0	0	0
$\sigma_{\alpha\alpha}$	up	32.0528	32.0557	-10.4441	-10.4670	-2.1000	-2.1188	0.3965	0.3927
	down	18.1345	18.1394	4.5979	4.5857	0.4217	0.4219	7.5403	7.5542
	max	32.0528	32.0557	10.8333	10.8228	1.0373	1.0368	7.5403	7.5542
	min	-29.9257	-29.9093	-10.4441	-10.4670	-2.1000	-2.1188	-8.6119	-8.6280
$\sigma_{\alpha\zeta}$	max	31.0936	31.0955	0	0	0	0	0.7090	0.7126
	min	-36.6918	-36.6841	-7.6042	-7.6306	-9.7470	-9.7618	-11.1936	-11.1882
$\sigma_{\zeta\zeta}$	up	1.0000	1.0000	1.0000	1.0000	1.0000	1.0000	1.0000	1.0000
	max	1.6056	1.5961	1.0000	1.0000	1.0000	1.0000	1.0154	1.0127

## V. CONCLUDING REMARKS

Various new zig-zag theories in displacement-based or mixed form, with a different representation of variables across the thickness and differently assumed zig-zag functions, so ultimately differently accounting for layerwise effects, or retaken from previous papers by the authors have been compared. Challenging elastostatic benchmarks with strong layerwise effects, under distributed or localized loading and simply-supported and clamped edges and with distinctly different material properties and thickness of layers, mainly in form of sandwich structures have been considered.

All zig-zag theories have the same five functional degrees of freedom like FSDT and HSDT (that in the cases here examined are very inaccurate), so the number of unknowns is independent from the number of constituent layers. To compare theories under the same conditions, the same trial functions and expansion order are used to obtain solutions in closed form.

The prefixed purpose was to show on a broader series of theories and benchmarks than in the former papers by the authors that whenever the expressions of coefficients of displacements are determined a priori by enforcing the fulfillment of the full set of interfacial stress compatibility conditions, of stress boundary conditions and of local equilibrium equations at a number of selected point sufficient to determine the expressions of all coefficients, the choice of the representation form and of zig-zag functions can be arbitrary without the results changing. When all these conditions are mutually occurring, it has been shown that zig-zag functions can even be omitted, with self-evident advantages from the computational standpoint.

Higher-order zig-zag theories, whose coefficients are redefined layer-by-layer by imposing the fulfillment of interfacial displacement and stress compatibility conditions, stresses boundary conditions at upper and lower bounding faces and local equilibrium equations at different points across the thickness proved to be always those most accurate and efficient, as a computational burden still comparable to that of ESL was required for all benchmarks. In particular, it was demonstrated that zig-zag functions can be freely chosen and variables can be assumed in an arbitrary form, i.e. different form one to another and from region to region across the thickness, without the results changing. According, a specific role does not need to be assigned to individual coefficients of displacements, being sufficient that the total number of coefficients to be determined corresponds to the number of conditions to be imposed. Consequently the expansion order of displacements can be freely chosen if this condition is met and at least it cubic/quartic.

In fact theories ZZA, ZZA\*, HWZZ, HWZZ\_RDF, ZZA\*\_43, HSDT\_34, HWZZM, ZZA-X1 to ZZA-X4 and ZZA-X1\* to ZZA-X4\* based on totally different forms of representation but satisfying the conditions mentioned above show indistinguishable results from each other and always prove to be the most accurate and efficient. The most efficient of all are

ZZA\*, ZZA\*\_43, HSDT\_34, ZZA-X1 to ZZA-X4 and ZZA-X1\* to ZZA-X4\* that omit the explicit presence of zig-zag functions, therefore they constitute a convenient option to much expensive 3-D finite element methods and discrete-layer models.

A partial fulfillment of above mentioned constraints implies instead that the accuracy decreases and becomes strongly depending on assumptions made. Lower-order theories HRZZ, HRZZ4, MHWZZA, MHWZZA4 and in particular ones that incorporate Murakami's zig-zag function MHR and MHR4 belong to this category. However in some cases they provide quite accurate results, but in general are rather inaccurate so, it is not possible to deduce any general rule about their usability. The only rule that can be drawn is that the higher-order zigzag theories of this paper with a redefinition of the coefficients obtained through the enforcement of the complete set of physical constraints are always accurate and efficient.

## REFERENCES

- [1] Y. Frostig, O.T. Thomsen, "High-order free vibration of sandwich panels with a flexible core," *International Journal of Solids and Structures*, 2004, vol. 41, pp. 1697-1724.
- [2] M.K.Rao, Y.M.Desai, "Analytical solutions for vibrations of laminated and sandwich plates using mixed theory," *Composite Structures*, 2004, vol. 63, pp. 361-373.
- [3] Y.Yang, A.Pagani, E.Carrera, "Exact solutions for free vibration analysis of laminated, box and sandwich beams by refined layer-wise theory," *Composite Structures*, 2017, vol. 175, pp. 28-45.
- [4] K.N.Cho, C.W.Bert, A.G.Striz, "Free vibrations of laminated rectangular analyzed by higher order individual-layer theory," *Journal of Sound and Vibration*, 1991, vol. 145(3), pp. 429-442.
- [5] E.Carrera, "A study of transverse normal stress effects on vibration of multilayered plates and shells," *Journal of Sound and Vibration*, 1999, vol. 225, pp. 803-829.
- [6] E.Carrera, "Developments, ideas, and evaluations based upon Reissner's mixed variational theorem in the modeling of multilayered plates and shells," *Appl. Mech. Rev.*, 2001, vol. 54, pp. 301-329.
- [7] E.Carrera, "Historical review of zig-zag theories for multilayered plates and shells," *Appl. Mech. Rev.*, 2003, vol. 56, pp. 1-22.
- [8] E.Carrera, "On the use of the Murakami's zig-zag function in the modeling of layered plates and shells," *Compos. Struct.*, 2004, vol. 82, pp. 541-554.
- [9] E.Carrera, A.Ciuffreda, "Bending of composites and sandwich plates subjected to localized lateral loadings: a comparison of various theories," *Composite Structures*, 2005, vol. 68, pp. 185-202.
- [10] L.Demasi, "Refined multilayered plate elements based on Murakami zig-zag functions," *Compos. Struct.*, 2004, vol. 70, pp. 308-316.
- [11] V.V.Vasilive, S.A.Lur'e, "On refined theories of beams, plates and shells," *J. Compos. Mat.*, 1992, vol. 26, pp. 422-430.
- [12] J.N.Reddy, D.H.Robbins, "Theories and computational models for composite laminates," *Appl. Mech. Rev.*, 1994, vol. 47, pp. 147-165.
- [13] S.A.Lur'e, N.P.Shumova, "Kinematic models of refined theories concerning composite beams plates and shells," *Int. J. Appl. Mech.*, 1994, vol. 32, pp. 422-430.
- [14] A.K.Noor, S.W.Burton, C.W.Bert, "Computational model for sandwich panels and shells," *Appl. Mech. Rev.*, 1996, vol. 49, pp. 155-199.
- [15] H. Altenbach, "Theories for laminated and sandwich plates. A review," *Int. J. Appl. Mech.*, 1998, vol. 34, pp. 243-252.
- [16] R.Khandan, S.Noroozi, P.Sewell, J.Vinney, "The development of laminated composite plate theories: a review," *J. Mater. Sci.*, 2012, vol. 47, pp. 5901-5910.
- [17] S.Kapurja, J.K.Nath, "On the accuracy of recent global-local theories for bending and vibration of laminated plates," *Compos. Struct.*, 2013, vol. 95, pp. 163-172.
- [18] J.N.Reddy, "Mechanics of laminated composite plates and shells: Theory and analysis (2nd ed)," 2003, Boca Raton: CRC Press.
- [19] W. Zhen, C. Wanji, Free vibration of laminated composite and sandwich plates using global-local higher-order theory, *Journal of Sound and Vibration*, 2006, vol. 289, pp. 333-349.
- [20] S. Kapuria, P.C. Dumir, N.K. Jain, "Assessment of zig-zag theory for static loading, buckling, free and forced response of composite and sandwich beams," *Composite Structures*, 2004, vol. 64, pp. 317-327.
- [21] V.N. Burlayenko, H. Altenbach, T. Sadowski, "An evaluation of displacement-based finite element models used for free vibration analysis of homogeneous and composite plates," *Journal of Sound and Vibration*, 2015, vol. 358, pp. 152-175.
- [22] L.Jun,H.Xiang, L.Li Xiaobin, "Free vibration analyses of axially loaded laminated composite beams using a unified higher-order shear deformation theory and dynamic stiffness method," *Composite Structures*, 2016, vol. 158, pp. 308-322.
- [23] U.Icardi, F. Sola, "Development of an efficient zig-zag model with variable representation of displacements across the thickness," *J. of Eng. Mech.*, 2014, vol. 140, pp. 531-541.
- [24] U. Icardi, A. Urraci, Free and forced vibration of laminated and sandwich plates by zig-zag theories differently accounting for transverse shear and normal deformability, *Aerospace MDPI*, 2015, vol. 5, pp. 108.
- [25] U. Icardi, A. Urraci, "Novel HW mixed zig-zag theory accounting for transverse normal deformability and lower-order counterparts assessed by old and new elastostatic benchmarks," *Aer. Sci. & Tech.*, 2018, vol. 80, pp. 541-571.

- 
- [26] M. Di Sciuva, "A refinement of the transverse shear deformation theory for multilayered orthotropic plates," *L'Aerot. Miss. & Spaz.*, 1984, vol. 62, pp. 84-92.
- [27] U. Icardi, "Higher-order zig-zag model for analysis of thick composite beams with inclusion of transverse normal stress and sublaminates approximations," *Compos. Part B*, 2001, vol. 32, pp. 343-354.
- [28] A. Catapano, G. Giunta, S. Belouettar, E. Carrera, "Static analysis of laminated beams via a unified formulation," *Compos. Struct.*, 2011, vol. 94, pp. 75-83.
- [29] A.G.de Miguel, E. Carrera, A. Pagani, E. Zappino, "Accurate Evaluation of Interlaminar Stresses in Composite Laminates via Mixed One-Dimensional Formulation," *AIAA Journal*, 2018, vol. 56, pp. 4582-4594.
- [30] W. Zhen, C. Wanji, "A study of global-local higher-order theories for laminated composite plates," *Compos. Struct.*, 2007, vol. 79, pp. 44-54.
- [31] U. Icardi, A. Atzori, "A. Simple, efficient mixed solid element for accurate analysis of local effects in laminated and sandwich composites," *Advances in Eng. Software*, 2004, vol. 35, pp. 843-859.



**AD Publications**

**Sector-3, MP Nagar, Bikaner,  
Rajasthan, India**

**[www.adpublications.org](http://www.adpublications.org), [info@adpublications.org](mailto:info@adpublications.org)**